Investigating the relationship between circulation patterns and cloudburst character in a changing climate

Sofia Litsmark

UPPSALA
UNIVERSITET

ABSTRACT

Investigating the relationship between circulation patterns and cloudburst character in a changing climate
Sofia Litsmark

The consequences of extreme weather in terms of heavy precipitation and flooding are devastating in both rural and urban areas. The cost on society to handle the damages are substantial. It is therefore of high interest to further investigate the mechanisms behind these extreme events. With a better understanding and future forecasting of heavy precipitation events (cloudbursts), the urban areas can adapt their infrastructure to future demands which would make the cities less vulnerable to flooding.

To better understand the mechanisms behind extreme precipitation scientists have studied North Atlantic atmospheric circulations and found a relation between those atmospheric circulations and cloudbursts in northern Europe. Furthermore, earlier studies have shown an indication of more frequent atmospheric circulation that causes cloudbursts in northern Europe in the future. Wei Yang at Swedish Meteorological and Hydrological Institute (SMHI) defined twelve new circulation pattern classes of North Atlantic scale, and this study aimed to investigate if there is a relation between those classes of circulation patterns and five empirical hyetographs generated by Olsson et al. (2017). This was accomplished by investigating what circulation pattern was present the day the cloudburst occurred. If a relation was found, the second objective was to see how the future frequencies of the circulation patterns would affect the distribution of hyetograph shape. To investigate future frequencies of the circulation patterns results from climate models were used.

The result showed an indication of a relation between circulation patterns and cloudburst character. The number of events was too small for any robust conclusions to be made, but tendencies were found, and further investigation could show more interesting results. Based on the assumption that the frequency of cloudbursts for each circulation pattern would stay the same in the future, the result in this study showed that the distribution of hyetograph shape would not change considerably in the future.

Key words: Circulation patterns, future climate, hyetograph, hyetograph shape, future rain patterns, cloudbursts

Department of Earth Sciences, Program for Air, Water and Landscape Science, Uppsala University, Villavägen 16, SE-75236 Uppsala, Sweden.

REFERAT
Undersökning av cirkulationsmönsters relation till hyetografkaraktär i ett framtida klimat
Sofa Litsmark

Konsekvenserna av extremväder, så som skyfall och översvämningar, är förödande för både landsbygd och urbana områden. Kostnaderna för samhället att reparera de skador som följer av översvämningar är ofta dyra och för att förebygga detta är det av intresse att vidare undersöka de mekanismer som styr extremväder. Med bättre förståelse och framtidsprognoser, kan städerna anpassa sin infrastruktur för de framtida utmaningarna.

Tidigare studier har visat att det finns en koppling mellan atmosfäriska cirkulationsmönster över Nordatlanten och extrem nederbörd i norra Europa. Studier visar även på att denna typ av cirkualtionsmönster kan bli vanligare i framtiden. SMHI definierade nylien tolv cirkulationsmönstersklasser på nordatlantisk skala och beskrev frekvensen av dessa idag och i framtiden. Syftet med denna studie var att undersöka om det fanns en koppling mellan de tolv cirkulationsmönstersklasserna och fem empiriska regntyper framtagna av Olsson et al. (2017). Historiska skyfall analyserades för att se vilket cirkulationsmönster som var dominant dagen då skyfallet inträffade. Vidare studerades frekvensen av cirkulationsmönster idag och jämfördes med frekvensen av samma cirkulationsmönster i framtiden. De framtida frekvenserna användes för att undersöka om det skulle bli någon förändring av fördelning av de olika regntyperna i framtiden. De framtida frekvenserna erhölls från simuleringar av framtida klimat med hjälp av klimatmodeller.

Resultatet från studien visade att det fanns en indikation till en koppling mellan vissa cirkulationsmönster och regntyper med en tidig regnintensitetstopp under regnhändelsen. Tyvärr var antalet regnhändelser för få för att med säkerhet kunna dra några slutsatser, men resultatet visade tendenser till kopplingar som bör undersökas vidare i framtiden. Baserat på antagandet att varje cirkulationsmönster kommer ha samma frekvens av skyfall i framtiden, visade det sig att förändringen av fördelningen mellan regntyperna kommer ändras med mindre än 1% mellan idag och 1971–2100. Utifrån resultatet går det därför inte att se någon tydlig förändring av fördelningen mellan regntyper i framtiden.

Nyckelord: Cirkulationsmönster, framtida klimat, klimat, skyfall, hyetograf, hyetografkaraktär, framtida vädermönster

PREFACE

This master thesis corresponds to 30 credits and is finalising the Master Program in Environmental and Water Engineering at Uppsala University and the Swedish University of Agricultural Science. The thesis has been conducted in collaboration with Tyréns AB, where Johan Kjellin has been supervising. Gabriele Messori has been subject reader and and Björn Claremar examiner, both at the Department of Earth Sciences, Program for Air, Water and Landscape Sciences, Uppsala University.

I would like to thank Jonas Olsson, Peter Berg, Johan Södling and Wei Yang at SMHI for providing me with data on the rain events, hyetographs and circulation patterns, and also for the useful input on my work. I would also like to thank Jimmy Olsson and Lars Marklund at Tyréns AB for their interesting thoughts and help during my work.

Sofia Litsmark

POPULÄRVETENSKAPLIG SAMMANFATTNING

Det framtida klimatet är något som debatteras flitigt i media. Hur kommer nederbördsmönstren se ut i Sverige om 50 eller 100 år, kommer regnen bli kraftigare eller kommer det regna oftare? För att för att få en aning om hur vädret kommer se ut i framtiden tittar forskare ofta på hur vädret har sett ut i medeltal, det vill säga att ett medelvärde av till exempel temperatur, nederbörd och vind tas fram för ett givet antal år tex 1979–2005, vilket kallas för 'dagens klimat'. För att sedan se hur det framtida klimatet kommer att se ut tittar forskarna på klimatmodeller som använder matematiska formler och fysikaliska samband för att beskriva land, hav, is och luft på vår jord. Dessa modeller räknar stegvis, till exempel timme för timme, ut förändringar i temperatur, nederbörd och vind i framtiden. Därefter beräknas ett medelvärde av alla klimatmodellernas resultat som kan jämföras med dagens medelvärden, för att se förändringar i framtiden.

Tidigare forskning har visat att det finns en koppling mellan storskaliga vädermönster och extrem nederbörd. Studier har även visat att de vädermönster som är kopplade till extrem nederbörd kan komma att öka i framtiden. Forskare vid SMHI definierade nyligen tolv klasser för vädermönster över Nordatlanten. Dessa klasser användes för att klassificera vädermönster för varje dag mellan 1997 och 2017. Därefter undersöktes frekvensen av dessa vädermönster i framtiden med hjälp av sex klimatmodeller som beskrev frekvensen av dessa vädermönster fram till år 2100. Med hjälp av denna information var det möjligt att se om det kommer bli någon förändring av vädermönster, och i förlängning regnmönster, i framtiden. Klimatmodeller är generellt dåliga på att simulera kraftig nederbörd då detta ofta är av lokal natur, därav analyserades endast frekvensen av cirkulationsmönster och utifrån den gick det att dra slutsatser om framtida regnmönster med avseende på extrem nederbörd.

Forskare vid SMHI har även analyserat historiska regnhändelser i Sverige för att finna karaktärsskillnader på regnen. Studien resulterade i fem regnkurvor som beskriver hur regnintensiteten är fördelad över tiden för händelseförloppet. Övergripande går det att säga att klass ett hade sin toppintensitet i den första femtedelen av tiden för regnhändelsen och klass två i den andra femtedelen av regnhändelsen och så vidare för de övriga tre klasserna. I Jimmy Olssons examensarbete undersöktes översvämningsdjup, i en liten småläsk ort, vid skyfall med regnkaraktärer som de fem empiriska regnkurvorna. Studien visade att de olika regntyperna gav signifikanta skillnader i översvämningsdjup. Det är därför av intresse att vidare undersöka om fördelningen av regntyperna kommer förändras i framtiden, det vill säga om de regn som ger störst översvämningsdjup kommer öka i framtiden. Syftet med denna studie är därför att undersöka om det finns en koppling mellan de fem regntyperna och de tolv vädermönstren.

I detta arbete undersöktes koppling mellan vädermönster och skyfallskaraktär genom att studera varje regnhändelse för sig för att se vilket vädermönster som rådde under den dagen skyfallet inträffade. Regnhändelserna var i en tidigare studie av SMHI kategoriserade i de fem regntypsklasserna och på så vis gick det att se om det fanns ett samband mellan regnkaraktär och vädermönster. Resultatet av denna studie visar att det är svårt att se någon koppling mellan vädermönstrets regnkaraktär då antalet regnhändelser har varit för få för att några slutsatser ska kunna dras. Däremot går det att se en tendens till en koppling

mellan vädermönster fyra, som innebär sydvästliga vindar i södra Sverige med ett lågtryck över Nordatlanten, och regn med sin toppintensitet i första tredjedelen av regnförloppet. Vidare undersöktes den framtida frekvensen av vädermönster för att undersöka om det kommer ske en förändring av frekvensen hos de olika regntyperna. Baserat på antagandet att det kommer vara lika vanligt att det blir ett skyfall för ett specifikt vädermönster idag som i framtiden, beräknades förändringen av fördelningen mellan regntyperna till mindre än 1% mellan idag och 2071–2100. Resultatet från studien visade därmed att fördelningen av regntyper inte kommer att förändras avsevärt i framtiden.

DEFINITIONS

Circulation pattern   Circulation patterns describe atmospheric configurations that can be seen repeatedly over time. They give an indication of what the atmospheric circulation looks like at a given time.

Cloudburst   Sudden and heavy precipitation. The definition by SMHI is "50 mm per hour or at least 1 mm per minute" (SMHI, 2017b).

Geostrophic wind   The direction and speed of geostrophic wind are determined by the pressure gradient force and the force caused by earths rotations, the Coriolis force. Geostrophic wind does not take into account the friction force from earth surface.

Hyetograph   A graph that describes the rain intensity over time for a rain event.

Return period for a rain event   A rain with, for example, a return period of 10 years refers to a rain with an intensity and volume of rain that only occurs every 10 years, according to statistics.

Subpolar (Icelandic) Low   A semi-permanent area of low pressure located in the North Atlantic Ocean centered over Iceland.

Subtropical (Azores) High   A semi-permanent area of high pressure located in the Atlantic Ocean, centered south of the Azores.

CONTENTS

1 INTRODUCTION

The future climate will increase the demands on our cities and their infrastructure. According to IPCC, heavy precipitation events in northern Europe are likely to increase in frequency, intensity or both, with some seasonal and regional variations (IPCC, 2013). Rapid urbanisation, complex infrastructure, and changes in the precipitation patterns caused by climate change are factors that make our cities more vulnerable to flooding (Willems et al., 2012). With a warmer climate the ability for air to hold moisture will increase, which could increase the frequency of cloudbursts (sudden and very heavy rainfall). According to Olsson et al. (2017) the total precipitation volume in Sweden will increase by 10–20% by the middle of this century, depending on the different emission scenarios. In most parts of Sweden the precipitation volume during wintertime (December–February) is about to increase, while the precipitation volume will decrease during the summer months (June–August) (Hernebring & Mårtensson, 2013).

Urban areas are sensitive to cloudbursts because of their impermeable surfaces that prevent infiltration of runoff water. This makes the urban areas dependent on their drainage systems. The drainage capacity in cities is limited and in the event of a cloudburst, the systems will overflow. The runoff water will instead find its way to low points in the landscape, called flood hazard areas (Hernebring & Mårtensson, 2013). In 2015 the insurance companies had 24.000 reported damages caused by flooding and the insurance claims ended up costing 1.046 million Swedish crowns (Elfström, 2015). Today it is not possible to prevent a cloudburst, but the urban areas can adapt their infrastructure to future demands so that they are suited for the vast amounts of water that a cloudburst entails.

In previous research, there have been attempts to find the relationship between circulation patterns and extreme events (e.g Yiou & Nogaj 2004, Pfahl & Wernli 2012, Cassou 2010). These studies looked at the two phases of the North Atlantic Oscillation (NAO+/NAO-), the "blocking" and the Atlantic ridge. Yiou & Nogaj (2004) found a relation between the NAO+ and increased precipitation extremes in northern Europe. Yiou & Nogaj (2004) also found, in their data from 1958 to 2003, that the last decade showed a more frequent occurrence of the NAO+, which could be an indication of more frequent cloudbursts in the future.

When studying cloudbursts, it is common to look at the hyetograph of the rain event, which describes the rainfall intensity over time. Olsson et al. (2017) studied the temporal distribution of rain intensity in extreme rain in Sweden between the years 1995–2004. This resulted in three groups of duration intervals with 5 hyetographs in each group. Olsson (2019) later studied the flood depth for each of the five hyetographs with a duration longer than 90 min. The study showed that the different hyetographs had great influence on flood depth when simulating a stationary rainfall. It is therefore of interest to further study the relation between these hyetographs and specific classes of circulation patterns.

To lower the cost on the society it is of great interest to improve the forecasting capabilities of these cloudbursts that may cause flooding. Therefore, it is important to understand the mechanisms behind these extremes (Pfahl & Wernli, 2012). Hence this study aims to increase the knowledge of cloudbursts relation to circulation patterns on a regional scale.

Furthermore, this relation may say something about the frequency and intensity of cloud-bursts in the future, based on climate models predictions about future frequencies of the circulation pattern.

1.1 AIM AND OBJECTIVES

This thesis aimed to investigate the relationship between five hyetographs and twelve North Atlantic atmospheric circulation pattern classes. The first objective was to investigate the relationship between the five national hyetographs, created by Olsson et al. (2017), and the twelve North Atlantic circulation patterns provided by SMHI. The second objective was to analyse the future frequency of these circulation patterns, which might say something about the frequency of these hyetographs in a future climate. Furthermore, this study can be seen as a pre-study for future research in this subject. This study aimed to answer the following questions.

- Is there a relationship between the five national type hyetographs and specific circulation patterns?

- Based on future frequencies of the circulation patterns, how will the frequency of those hyetographs change?

1.2 DELIMITATION

This study is based upon data from an earlier study by SMHI that only used data until year 2004. This study is limited to only look at future atmospheric circulations patterns based on the emission scenario of RCP 8.5, further explained in section 2.6.

2 BACKGROUND

2.1 PRECIPITATION AND CLOUDBURST

Precipitation is created through condensation of water vapor. Humid air rises and at a lower pressure the air expands and cools down. Eventually, the vapor condenses on small particles in the air, called cloud condensation nuclei, and fall as precipitation (Liljequist, 1970). The vertical movement of air is generated by three main processes, which divide rain into three categories, orographic, frontal and convective rain. Orographic rain, occurs when wind forces air up a slope. The lower air pressure up the hill will cause a lower temperature and water vapor will condense into raindrops (Met Office, n.d.c). Orographic rain can also occur in coastal regions where faster winds from the sea are lifted above the slower moving air on land. In Sweden, the maximum precipitation from this kind of rain falls approximately 10–20 km inland from the coastline (Svenskt Vatten, 2011).

Frontal rain occurs when two air masses with different properties in terms of temperature and moisture collide (Olsson et al., 2017). Depending on where this air mass is created it will have different properties. Air masses created over continents are generally dryer and colder (in winter) than air masses created over oceans because they have an unlimited supply of moisture. Nature is constantly trying to find balance and therefore winds try to spread the heat from the equator to the poles and vice versa. When the air masses collide they move along each others fronts and a cyclone is formed (SMHI, 2015a). A cyclone is a large system of winds that rotates (counterclockwise in the northern hemisphere) around the center of a low atmospheric pressure. The diameter of a cyclone of this magnitude is 1 000–2 000 km. When the warm air mass catches up on the cold air mass it is forced to move upward on top of the cold air mass and as a result there will be showers in front of the warm front (Svenskt Vatten, 2011). In the Northern Hemisphere, there is a natural movement of air from west to east caused partly by the rotation of the earth and partly by the differences in temperature (Svenskt Vatten, 2011). Cyclones created over the North Atlantic Ocean are usually moving from west to east because of this natural movement of air (SMHI, 2017a). This phenomenon also has an effect 8–11 km above ground where it creates a core of strong winds blowing from west to east, called the Jet stream (Met Office, n.d.d). The jet stream meanders over the northern hemisphere and may affect the atmospheric circulation patterns (SMHI, 2017a).

The third category of rain is the convective rain. This occurs when the sun heats the ground which further heats the layer of air closest to the ground. The air closest to the ground becomes warmer than the surrounding air and starts to rise while cooler air will replace its position on the ground. When the warm air rises it cools of and condenses into rain drops that will start to fall. Rain of this kind is common inland during summer when the sun heats the ground and air can pick up enough moisture from surrounding lakes and damp grounds (Olsson et al., 2017). Convective rain is usually local and depends on relatively fast atmospheric circulations and is therefore difficult to predict (Svenskt Vatten, 2011). There is always an element of convective rain when a cloudburst occurs in Sweden. Due to higher temperatures during summer, cloudbursts in Sweden are most common during the summer months (Olsson et al. 2017, Svenskt Vatten 2011).

In Sweden, rain intensity varies regionally and recent research, performed by SHMI, made

it possible to divide Sweden into four cloudburst regions, Southwest, Southeast, Central and North. According to the same research, the north of Sweden had the lowest intensities while the southwest of Sweden had the highest (Olsson et al., 2017). Olsson et al. (2017) suggests that this difference is due the fact that the west coast of Sweden is affected by air masses from the subtropics, that are warmer and can pick up more moisture on their way over the Atlantic Ocean and therefore has the highest rain intensities. Dry and warm air masses from Finland and Russia can pick up moisture on their way over the Baltic sea. While air masses form the Norwegian sea and over the Scandinavian mountains do not have the same thermal capacity, which explains the more intense cloudburst in the South of Sweden compared to the North. Olsson et al. (2017) pointed out that even though there are some regional differences in frequencies of heavy precipitation, cloudbursts could occur in all regions of Sweden (Olsson et al., 2017).

2.1.1 Definition of cloudburst

According to SMHI, the definition of a cloudburst is a rain event with an intensity of "50 mm per hour or at least 1 mm per minute" (SMHI, 2017b). The other Scandinavian countries have different ways of defining cloudburst. In Denmark, the definition is "at least 15 mm in 30 minutes" (DMI, 2017). This is corresponds to a rain with a return period of 3 years in Southwest of Sweden. In Norway, there is no clear definition but since the landscape is highly diverse, it could be preferable to use different definitions of cloudbursts in different regions. In Finland, the definition of a cloudburst is "at least 30 mm within an hour" which corresponds to a return period of 30 years for the central region of Sweden (Olsson et al., 2017).

The Swedish definition of "50 mm per hour or at least 1 mm per minute" was first evaluated in a report by Olsson & Josefsson (2015), where the authors pointed out that the criteria "50 mm per hour" only occurred nine times in SMHI´s rain data during the period 1996—2017. The second part of the definition was not evaluated in the report from 2015 but in 2017 the time resolution of the data had improved and Olsson et al. (2017) used the definition "15 mm in 15 minutes". The authors found that a rain event with an intensity of 1 mm in 1 minute is very common and corresponds to a rain event with a return period of 0,5 years, while 50 mm per hour in the analysed data corresponded to a return period of more than 100 years. Olsson et al. (2017) suggest that a simplification of today's definition would be preferable and the suggestion they presented was "at least 15 mm in 15 minutes at any time during the rain". This definition would correspond to a rain event with a return period of 10 years, for all four regions in Sweden (Olsson et al., 2017).

2.2 CIRCULATION PATTERNS

Circulation patterns describe atmospheric configurations that can be seen repeatedly over time (Cassou, 2010). They give an indication of what the atmospheric circulation looks like at a given time. Depending on how the circulation patterns are calculated the number of patterns may vary.

Circulation patterns are traditionally calculated with clustering methods. One way is to iteratively execute the classification from randomly selected samples from the data set and then cluster them into a given number of clusters K, see section 2.5 for a more detailed de-

scription of the method. Circulation patterns are classified based on their mean conditions (Cassou, 2010). The input variables can be daily mean sea level pressure from reanalysis data e.g. ERA-interim (ECMWF Re-Analysis Interim). The output is the different circulation patterns based on the given number of clusters. In a paper by Christiansen (2007), the vulnerability of applying the wrong number of clusters is pointed out. Applying a unsuitable number of clusters for the data can make the algorithms detect multiple clusters in unimodal data (Christiansen, 2007). Unimodal data should only have one cluster and if it is forced into several clusters the result can show trends that are false. It is therefore important to investigate the choice of number of clusters thoroughly. Wei Yang (2019) at SMHI defined the 12 circulation patterns (clusters) used in this report. The decision of using 12 clusters was, according to Wei Yang (2019) based on an internal investigation of the optimal number of clusters at SMHI.

The circulation patterns used in this study are calculated based on the concept of Fuzzy sets, which is a method that describes the "level of belonging" for a certain statement. Therefore the method does not tell the exact truth but the degree of truth. This method uses imprecise statements to describe the circulation patterns (Bardossy & Samaniego, 2002). Usually, the real world is not black or white, more like a scale of gray, and this is when fuzzy logic is a good complement.

When studying the atmospheric circulations at the North Atlantic scale, the most commonly used circulation patterns are: The North Atlantic Oscillation (NAO) with its two phases, the "blocking" and the Atlantic Ridge. The different phases of NAO gives an indication of the most likely pressure set-up that can be expected during upcoming months. A positive NAO indicates that the pressure differences over time between the Subtropical (Azores) High and the Subpolar (Icelandic) Low, is high. A high pressure difference indicates that there will be strong westerly winds over the North Atlantic (Liljequist, 1970). Which typically gives warm winters in south and central Europe since warm air form the North Atlantic Ocean will advance over this area (Met Office, n.d.a). A negative phase of the NAO gives, on the other hand, less strong westerly winds over the North Atlantic due to lower differences between the Subtropical High and the Subpolar Low. This allows easterly wind from Russia to advance over Europe and during winter the easterly winds are cool and dry which generates a cold winter over Northern and central Europe (Met Office, n.d.a). The North Atlantic circulation patterns during the cold months, October–April, are shown in figure 1. The coloured areas represent how much the conditions deviate from average conditions, positive (red) and negative (blue). The lines and numbers in the figure indicates where and at what height the air pressure is 500 hPa. The top 2 figures represent the two phases of NAO (NAO+ and NAO-) and the bottom two represent the Blocking circulation pattern to the left and the the Atlantic Ridge circulation pattern to the right.

Figure 1. The most commonly used north Atlantic circulation patterns associated with cold months, October–April. The lines and numbers in the figure indicates where and at what height the air pressure is 500 hPa. In the figure the positive NAO pattern is associated with a blue outline, negative NAO with green, Euro-Atlantic blocking red and the Atlantic ridge pattern with violet (ECMWF, 2015).

The North Atlantic circulation patterns are a bit shifted during the warm season, May–September, these can be seen in figure 2. They are represented in the same order as in the figure above. A positive phase of the NAO during summer generates warmer and drier conditions than the negative phase of the NAO that generates cooler and wetter summers in northern Europe (Met Office, n.d.b).
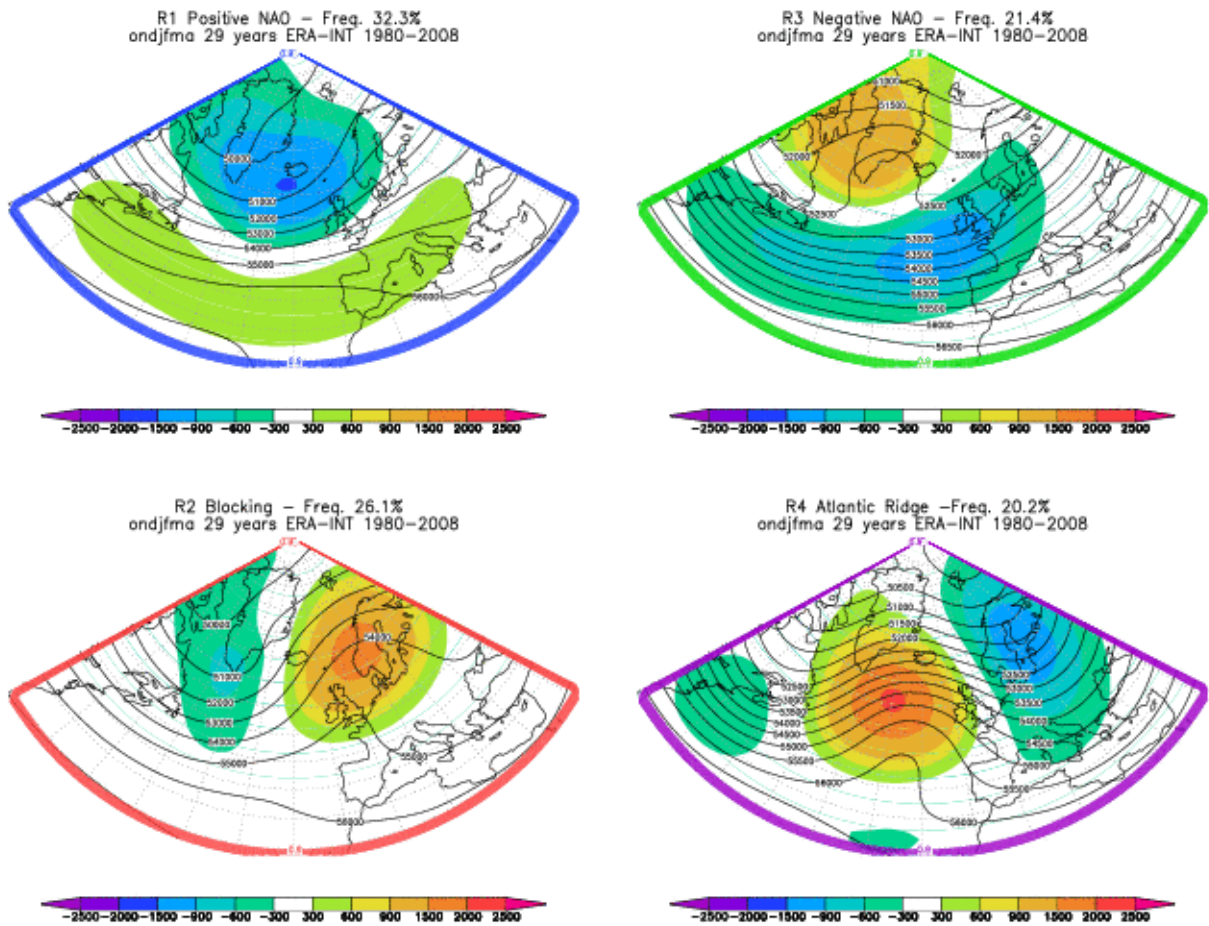
6
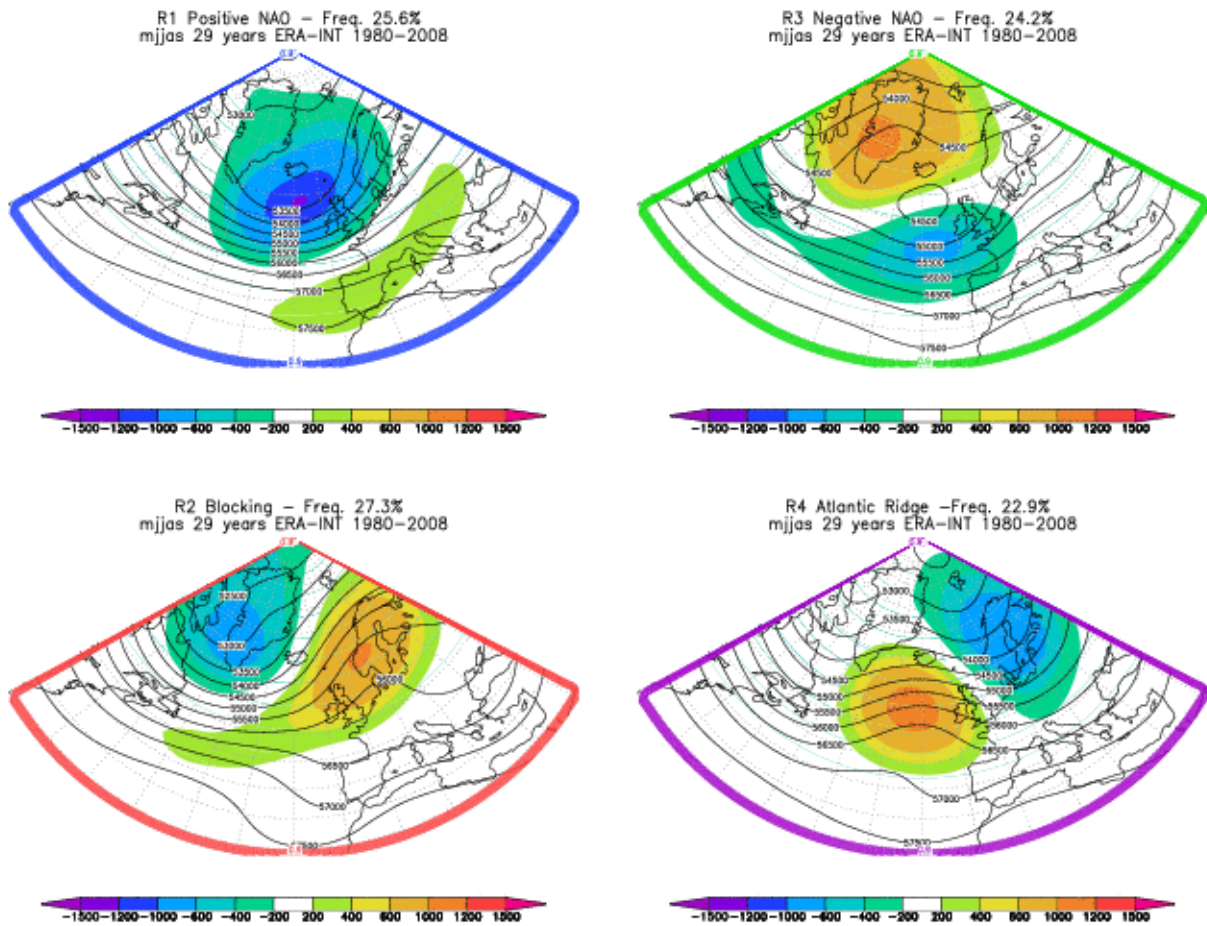
Figure 2. The most commonly used north Atlantic circulation patterns associated with warm months, May–September. The lines and numbers in the figure indicates where and at what height the air pressure is 500 hPa. In the figure the positive NAO pattern is associated with a blue outline, negative NAO with green, Euro-Atlantic blocking red and the Atlantic ridge pattern with violet (ECMWF, 2015).

2.3   CLOUDBURSTS' RELATION TO CIRCULATION PATTERNS

Yiou & Nogaj (2004) presented a new synthetic way of mapping the impact of atmospheric regimes on climatic extremes. According to the report, heavy precipitation over Northern Europe and the Eastern United States was associated with the NAO+ regime, while the NAO- regime was associated with heavy precipitation over Southern Europe and the Canadian Arctic. The "blocking" regime gave, according to the research heavier precipitation over Eastern Greenland and the Mediterranean. It should be noted that the east coast of southern Sweden differs from the rest of Sweden and had its precipitation highs when the NAO- was the dominant regime. The result from the report also showed that the Atlantic ridge regime had little effect on the precipitation maxima over the North

Atlantic–European region. Yiou & Nogaj (2004) also found, in their data from 1958–2003, that the last decade showed more frequent NAO+ episodes, which corresponded to high winter temperatures as well as high precipitation rates in Northern Europe and the Eastern United States. Their research was limited to only analyse the winter months (December–February) and it should be noted that most cloudbursts in Sweden occur during mid and late summer (Olsson & Josefsson, 2015).

Another study on circulation patterns was performed by Pfahl & Wernli (2012), who studied the occurrence of cyclones when there was a precipitation extreme. From the result, one could see that Sweden had a relative frequency of 20–30% cyclones in the ERA-Interim data during 1989–2009. The study used satellite-based precipitation estimates as a reference for the precipitation extremes. The corresponding percentage of 6-hourly precipitation extremes occurring simultaneously with a cyclone at the same grid point was 70–80% in Sweden (Pfahl & Wernli, 2012). The same report pointed out that the frequency of precipitation extremes related to a cyclone was higher during the summer period (June–August) in Sweden (Pfahl & Wernli, 2012). This result agrees with research conducted by Olsson & Josefsson (2015), that found July to be the month of the year with the most frequent occurrence of cloudbursts.

Consistently with previous research (e.g. Yiou & Nogaj 2004), Cassou (2010) studied the relation between atmospheric circulation patterns and extreme weather using the same four circulation patterns and the study was limited to only analysing winter months (December–February). Cassou (2010) pointed out that there was a strong relationship between circulation patterns and precipitation extremes. To find the extremes the author looked at the 95-percentile of daily mean precipitation values and the result showed that the NAO+ favored precipitation extremes in northwestern Europe.

In a study on Swedish precipitation extremes, an extreme precipitation event was defined as an event with >40 mm of observed daily precipitation (Hellström, 2005). The classification of the weather types was based on the Lamb method (Lamb, 1972) and resulted in 27 different weather types (circulation patterns) on a local scale over Scandinavia. The result showed that it was important to separate cyclonic and purely frontal precipitation when analysing heavy precipitation. Furthermore, the result showed that extreme rain events in Sweden were favoured by southerly winds. The author concluded that the cyclonic weather types were the most common ones connected to extreme precipitation. The author suggests this is due to higher vertical velocities and slightly higher moisture content for this weather type (Hellström, 2005).

2.4 EMPIRICAL HYETOGRAPHS

Hyetographs represent the relationship between rain intensity and duration. Olsson et al. (2017) studied the temporal distribution of rain intensity in extreme rain in Sweden. The rain events were categorised based on their duration: ≤ 60 min, 60–90 min and ≥ 90 min. From historical data from rain gauges, the authors used K-mean cluster analysis to generate the hyetographs. The K-mean cluster analysis bases its algorithm on putting N data into K clusters (MacKay, 2003). See section 2.5 for a more detailed description of the method of K-mean clustering.
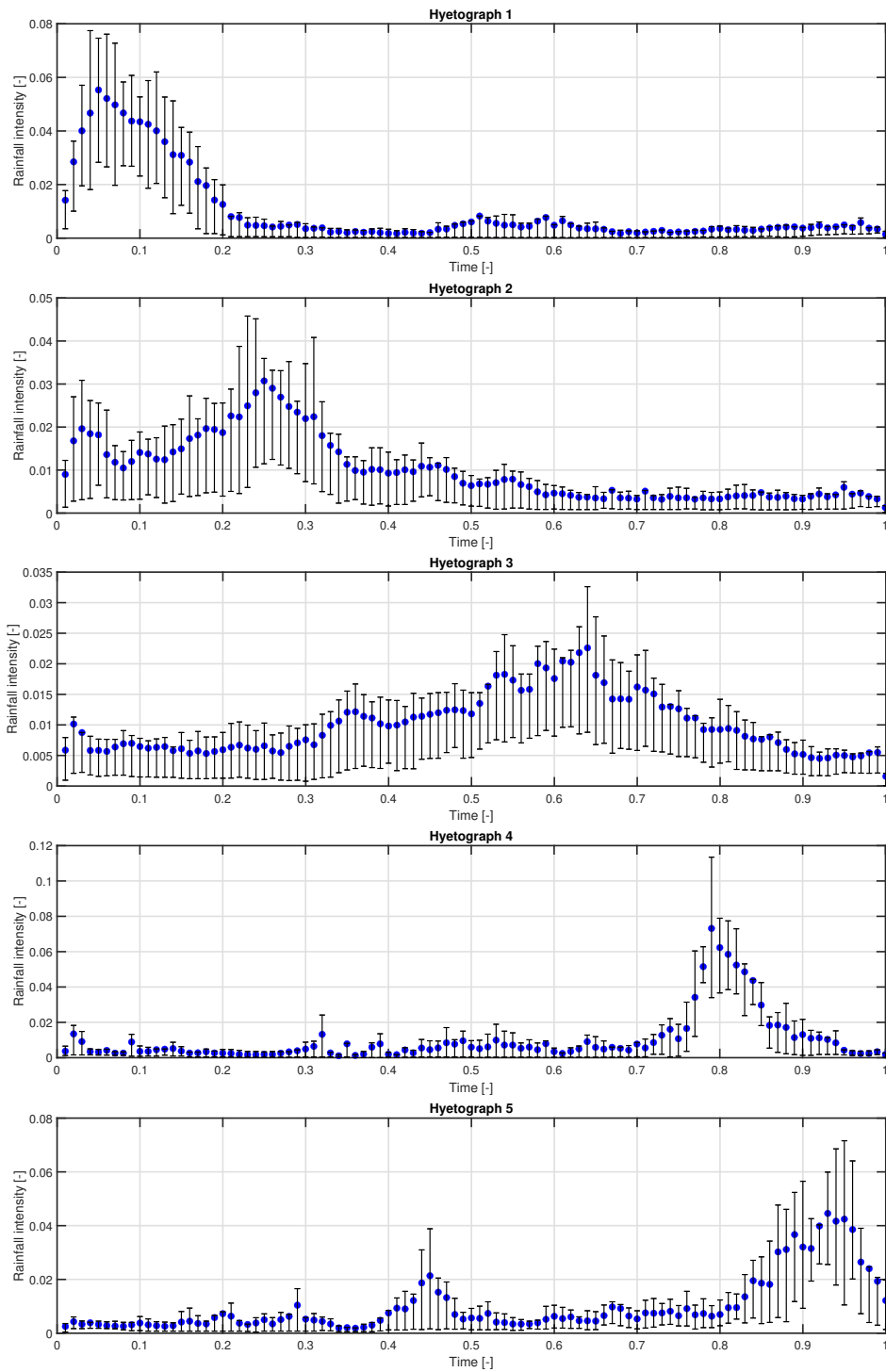
Figure 3. The national hyetographs generated by Olsson et al. (2017) for cloudbursts with a duration longer than 90 min. The blue dot marks the mean value while the whiskers show the dispersion of the value on the Y-axis.

In the analysis conducted by Olsson et al. (2017) they used five clusters, which generated

five hyetographs for each duration class. The rain events were then normalised over both duration and total flood depth. With this approach, all graphs have the same number of intensity values, but are distributed differently depending on how pointy the peak was and the arrival of the peak. To extract the interesting data from the historical rain data set, Olsson et al. (2017) decided to define a cloudburst as an event where the rain intensity was "at least 1 mm per minute" at some point during the rain event. Figure 3 shows the resulting hyetographs for a duration longer than 90 minutes. They are numbered based on the arrival of the peak.

From the graphs, one can see that the peak of the intensity varies in steepness and arrival of the peak. To obtain the rainfall intensity, the mean value (blue dot) can be multiplied by the total volume of rainfall. Table 1 show the distribution of the different duration classes and hyetograph shapes. Notice that each hyetograph has its individual scale on the y-axis.

Table 1. Distribution of hyetograph shape of the rain events in %. The total number of rain events is shown in the right column.

Duration time	Hyetograph shape					Total number of
[min]	1	2	3	4	5	rain events
>90	18.2%	27.3%	40.1%	6.1%	8.3%	132

Olsson (2019) studied these hyetograph´s relation to flood depth. The hyetographs were regenerated for at rain event with a duration of 120 min. He used a 2D surface model of an urban catchment that he coupled with a 1D model of the drainage network to evaluate the flood depth in depressions in the landscape and where the drainage system overflows and causes floods. Olsson (2019) evaluated the flood depth when simulating a cloudburst with a return period of a 100 years. The study showed that hyetograph 1 followed by hyetograph 2 gave the largest flood depth in all 10 evaluation points, while hyetograph 3 gave the lowest flood depth for the same scenario. The flood depth for hyetograph 2 and 5 varied within the evaluation points and did not show a consistent pattern. He compared these with the most commonly used rain scenario when modeling hydrology in Sweden, the Chicago design storm (CDS) (Svenskt Vatten, 2011). Olsson (2019) concluded that the only hyetograph that could match the flood depth of the CDS rain, in his case study, was hyetograph 1. Furthermore, this result indicated that the method used for hydraulic modeling in Sweden seems to overestimate the flood depth. Therefore, it is of interest to investigate if there will be heavier rain events in the future or not, which is a second objective of this thesis. Table 2 show the flood depth in each evaluation point Olsson (2019) used when simulating a stationary rain.

Table 2. Maximum flood depth, in cm, at the evaluation points when simulating a stationary rain event.

	Flood depth [cm] at evaluation point:									
Scenario	A	B	C	D	E	F	G	H	I	J
Hyetograph 1	43	34	38	50	41	29	41	37	30	29
Hyetograph 2	38	32	34	44	30	23	32	24	22	25
Hyetograph 3	34	30	31	39	22	16	25	23	18	23
Hyetograph 4	39	33	36	48	41	26	36	27	28	28
Hyetograph 5	36	31	33	43	37	21	29	24	23	25
CDS	45	34	39	51	42	28	42	37	31	31

2.5   K-MEAN CLUSTERING

The K-mean cluster analysis bases its algorithm on putting N data points into K clusters (MacKay, 2003). It is a iterative method and the number of clusters is predefined by the user. The optimal number of clusters varies depending on the data set and it is crucial for the robustness of the resulting variation within the clusters (Christiansen, 2007). The aim is to have as low variation as possible within the clusters but still avoiding to many clusters. Using the same number of clusters as data point in the data set gives the lowest variation but in that case the clustering method looses its objective. The method is generally based on the following steps:

1. First the number of clusters K is defined and each cluster is assigned with a centroid, c_1-c_K. The centroids are randomly selected within the data set of N points.

2. For each data point, x_1-x_N, the distances to the centeroides are calculated and each data point will be assigned to the nearest cluster. The distance can be calculated in several ways depending on the type of data set, e.g. Euclidean.

3. When each point have been assigned a cluster, the cetroids c_1-c_K are recalculated based on the data points that have been assigned to the specific cluster.

4. Step 2 and 3 are repeated until the data points stop changing cluster membership. Then the optimal clustering based on the selected number och clusters has been achieved.

To evaluate the robustness of the clustering several methods can be used and generally the methods evaluate the variance within the clusters. In MatLab for example, there is a function called Silhouette plot that can be used to evaluate the robustness of the clustering and this plot gives an indication of what is the most suitable number of clusters for the given data (MatLab, n.d.).

2.6   CLIMATE MODELS

To be able to perform analysis on the the climate a 3-dimensional model is needed, that can mathematically describe the atmosphere, land surface, oceans, lakes, and ice (SMHI, 2019). Earth is divided into grid cells and each cell is given hydrological and meteorological variables such as wind, precipitation, and temperature. These grid cells extend in the

vertical, with grid cells stacked on top of each-other in the atmosphere and if it is placed where there is ocean the grid cells extend down into the ocean. The grid cells closer to the earth's surface are usually thinner than the ones further out in the atmosphere, because there are more molecules closer to the surface and therefore it is more interesting to have higher spatial resolution there. The same for the cells reaching down into the oceans. Based on laws of physics the calculations are carried out with time steps of, for example, 15 min and then running the calculations for 100 years, therefore a lot of computing power is necessary. When looking at the whole climate (Global Climate Models, GCM) the grid cells have a resolution of 100–300 km. Sometimes a higher resolution is required and a downscaling from the GCM necessary. For this a Regional climate model is applicable and the grid is placed over a smaller area with a resolution of 50 km or less. The Regional model looks at the global model to see what happens outside the grid. This is usually called a downscaling. The computing power need for a regional model is generally much less than for a global climate model (SMHI, 2019).

To describe different scenarios of concentrations of greenhouse gases in the atmosphere by 2100, the IPCC calculated four 'Representative Concentration Pathways' (SMHI, 2019). The RCP 8.5 represents the scenario with the highest greenhouse gas emissions and is sometimes called the 'high-emission business as usual scenario' (Riahi et al., 2011). RCP 8.5 represent the pathway where earth would end up with radiative forcing of 8.5 W/m^2 more than pre-industrial revolution.

The RCP 8.5 scenario is based on the following assumptions (Riahi et al., 2011):

- Increased population, leads to more land taken under humanity
- Relatively slow economic growth with slow but forward-moving technological improvements
- This leads to ineffective and high energy demands
- High dependence on fossil fuel
- Absence of climate actions in politics
- Increased carbon dioxide emissions
- Increased methane emissions

2.6.1 Climate models used in this study

The climate models used in this study were chosen by Wei Yang and Peter Berg at SMHI. They are listed below with their names and where they are developed (IPCC, 2013). Within each climate model there are components that describe the different elements, such as atmosphere, ocean, sea ice and land surface. It differs between the models which type of equations or models they use to describe these elements, see table 3 . For example, they all have different models to describe the atmosphere and the top grid in the models differs between 10–0.01 hPa (IPCC, 2013), which represents the atmospheric pressure at an altitude of 32–64 km above sea level respectively.

Table 3. The climate models used in this study, chosen by Wei Yang and Peter Berg at SMHI, are presented in this table together with where they are developed and what model component that are included in the climate models (IPCC,2013)

| Climate model | Developed by: | Model components | | | | |
		Atmosphere chemistry	Land surface	Ocean	Ocean biochemistry	Sea ice
NorESM1-M	Norway	-	X	X	-	X
MPI-ESM-LR	Germany	X	X	X	X	X
IPSL-CM5A-MR	France	X	X	X	X	X
HadGEM2-ES	UK	-	X	X	X	X
EC-EARTH	Europe	X	X	X	-	X
CNRM-CM5	France	-	X	X	X	X

3 MATERIAL AND METHOD

Data for the project was provided by SMHI and the analysis was carried out using Matlab. The following section describes the method SMHI used to collect and analyse the rain data. This section also describes how the selection of rain gauges to use in this study was made and the reasoning behind the decisions. Furthermore, this section describes how Wei Yang at SMHI defined the circulation patterns used in this study.

3.1 EXTRACTING RAIN EVENTS

For a rain event to be classified as a cloudburst it had to meet the specific criteria, and the following routine was used by Olsson et al. (2017) to extract these events from the rain data provided by the municipalities in 15 cities in Sweden.

1. Identify rain data with a gap of $\geq$1 hour between the data points, these were seen as breakpoints between the events.

2. Divide the data into sets based on the breakpoints.

3. Transform the data to mm/min.

4. Identifying the first and last data in each set that has a mean intensity of 1 mm in 60 min, to have a start and end of the rain.

5. Calculate the mean intensity for the rain, if the mean intensity is $\leq$0,1 mm/min the event is rejected.

6. Save the events that meet all criteria in a separate file.

The events were then sorted into classes depending on their duration, 0–60 min, 60–90 min, and 90+ min. For each of the classes, the following operation was performed.

1. Collect all events within the desired class.

2. Normalise the duration time of each event so that the time axis goes from 0 to 1.

3. Calculate the total volume for the event and normalise the volume for the event so that the y-axis goes from 0 to 1.

4. Sample the event in 100 points along the dimensionless time axis.

To divide these extreme rain events into groups, K-mean clustering analysis was applied (MacKay, 2003), using groups for each class Olsson et al. (2017). To be able to relate the result in this study to Olsson (2019) study, only the five hyetographs with a duration of $\geq$90 min were analysed. The rain events are therefore the same as in Olsson et al. (2017) and have already been categorised into the different hyetograph shapes. To improve the number of rain events an idea was to use rain events from all three classes, 0–60 min, 60–90 min, and 90+ min, but due to the fact that their hyetographs are not identical this merging could not be carried out. For example, hyetograph 4 for the duration classes 60–90 min and 90+ min differ a lot in terms of rain intensity of the peak even though the arrival of the peak (when normalised) is almost the same. This was another reason for only using the rain events in the 90+ min class.

3.2 RAIN GAUGES

The rain data used in the SMHI report 47 and later in this study was collected by municipalities using a rain gauge of the model tipping bucket (Olsson et al., 2017). A rain collector of this kind is equipped with two "buckets" that collects the rain, usually 0.1 or 0.2 mm, until it is full and the bucket will tip over. The other bucket will start collecting precipitation and a sensor detects the movement. The number of tippings during a specific time period corresponds to the intensity of the precipitation (Olsson et al., 2017). Data in this study is based on the data used in the report by Olsson et al. (2017). The start and end date for each rain gauge is found in table 4.

Table 4. Start and end date for each rain gauge at the different locations (Olsson et al., 2017)

Location	Start date	End date
Borås	April 1982	Juni 1994
	Feb 1988	Aug 2004
Göteborg	July 2000	Oct 2004
Halmstad	Jan 1992	Feb 2004
Helsingborg	Jan 1991	April 2004
Jönköping	Sept 1985	Aug 2004
Kalmar[1]	Oct 1991	Nov 2004
Karlskrona	Feb 1998	Oct 2004
Karlstad	Dec 1995	Sept 2004
Malmö	April 1980	Aug 2004
Skellefteå	Nov 1996	Sept 2004
Stockholm[2]	Jan 1984	Dec 2004
Sundsvall	Maj 1991	Sept 2004
Uddevalla	Jan 1993	Aug 2004
Uppsala	June 1991	Nov 2004
Växjö	June 1985	Aug 2004

[1] Many interruptions in the Kalmar rain series. Some of the data has been replaced with data from other rain gauges in the municipality .

[2] Interruptions in Torsgatan´s rain series have been replaced with data from other stations. All of 1994 is missing.

After a discussion with Peter Berg and Wei Yang at SMHI, Skellefteå and Sundsvall were excluded from the analysis, since their geographical locations caused them to have different precipitation patterns connected to the circulations patterns than the other locations. This was found in an internal investigation by SMHI. Their influence on the analysis could, therefore, shift the relation between the hyetographs and the circulation patterns, and a clear relation would be harder to find. To avoid this problem Skellefteå and Sundsvall were excluded from the analysis.

To avoid the potential problem with the varying lengths of the time series, several attempts were made to find the time interval that would cover the most rain events. In Appendix B figure B.2 illustrates the distribution of hyetograph shape for 5 rain gauges with running periods from 1985–2004. These graphs are similar to the graphs presented in figure 8, that has the time period of 1996–2004, even though they have different time frames, 20 years and 8 years respectively. The time period that was found to cover the most rain events was 1996–2004, with 76 rain events. The rain gauges in Göteborg and Karlskrona were therefore excluded from this study because of their short running periods. Apart from Sundsvall, Skellefteå, Karlskrona and Göteborg all stations in table 4 were used for this analysis, summing up to 11 stations. Table 5 summarises the number of rain events that were analysed, and their distribution over the different hyetograph shapes.

Table 5. Distribution of hyetograph shape of the rain events. The total number of rain events is shown in the right column.

Duration time [min]	Hyetograph shape					Total number of rain events
	1	2	3	4	5	
>90	16	24	24	5	7	76

3.3 CLASSIFICATION OF CIRCULATION PATTERNS

Based on the concept of fuzzy sets, Wei Yang in collaboration with Peter Berg, both at SMHI, defined the circulation patterns classes used in this study. They used a method that made the circulation pattern classes tailored for the location, in this case mid and south of Sweden, and therefore they did not produce the more common number of circulation patterns, 4 (as explained in section 2.2. As explained earlier the decision of using 12 circulation pattern classes was, according to Wei Yang (2019), based on an internal investigation of the optimal number of classes at SMHI.

The calculations were based on daily mean sea level pressure (MSLP) from the ERA-Interim (0.75°x 0.75°) 6-hourly data, from 1979–1997. As a predictor of classification, the data were gridded at a 3° instead of their original grid. The circulation patterns are described as maps with lines that are numbered and show where and how much the conditions, in this case sea level pressure, depart from average conditions. The resulting anomaly maps of each circulation pattern class can be seen in figure 4. The maps only give an indication of what the pressure set up might look like for the days that have been classified into the different classes of circulation patterns, the actual pressure set up can be a bit shifted. For each day, between 1979–2017, Wei Yang determined what circulation pattern was present. For the days that did not match one of the 12 circulation patterns a 13th circulation pattern class was used. This class does not have a defined anomaly map of the circulation pattern. The data set with the number of the present circulation pattern for each day is the data set that has been used for the analysis in this report.
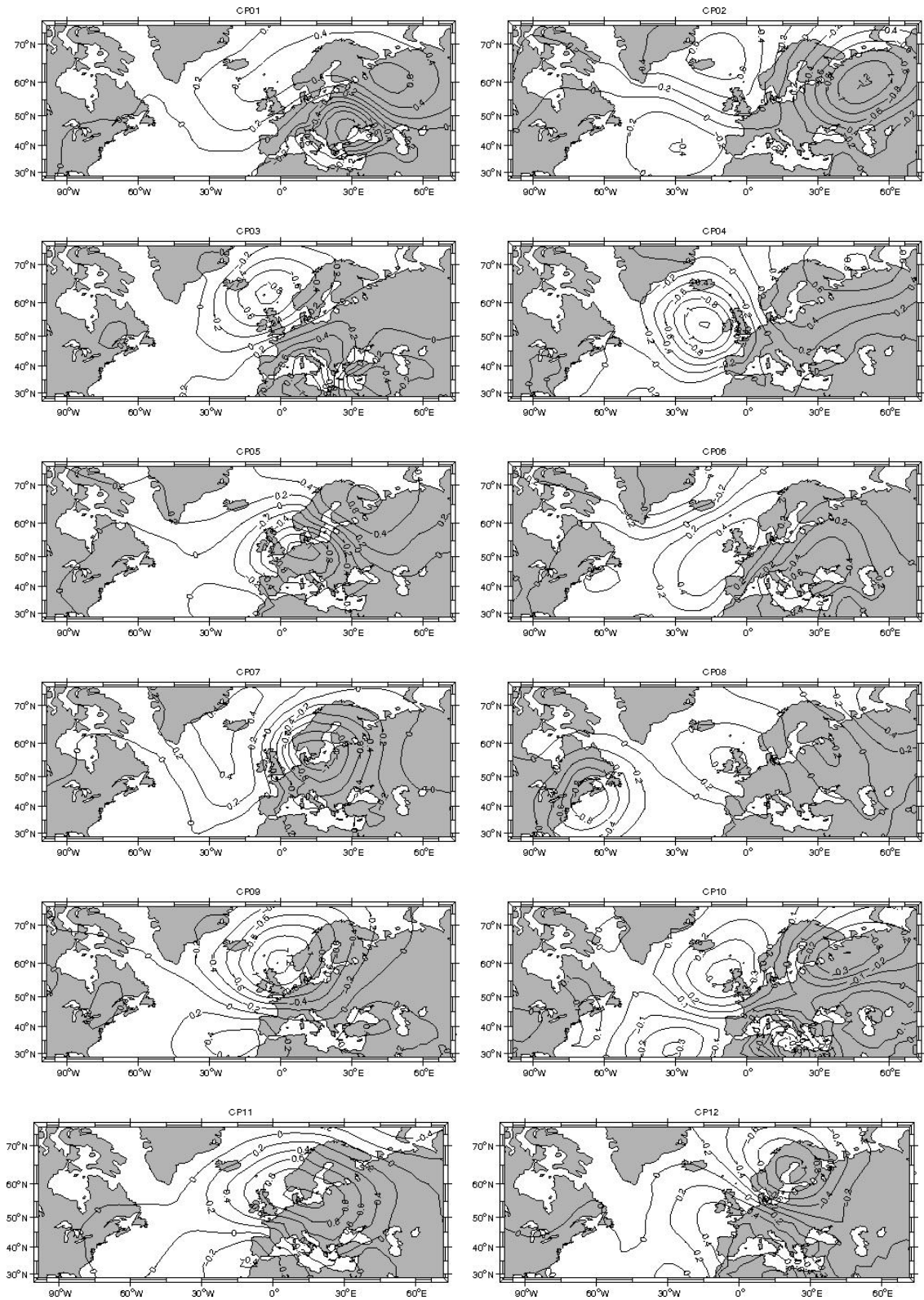
Figure 4. Anomaly maps of circulation patterns created by Wei Yang at SMHI. The numbers on the side of the figures show the longitude and latitude in degrees for orientation. The numbers on the lines in the figure corresponds to how much the conditions depart from average conditions in that area, the numbers are unitless standard deviations based on sea level pressure.

17

The dominant geostrophic wind directions in south of Sweden for each circulation pattern is shown in table 6.

Table 6. Dominant geostrophic wind direction in south of Sweden for each circulation pattern.

Circulation pattern	Dominant geostrophic wind direction
1	Southeasterly
2	Northeasterly
3	Southwesterly
4	Southwesterly
5	Easterly/Southeasterly
6	Northerly/Northeasterly
7	Easterly
8	Northerly
9	Southwesterly
10	Northerly
11	Northwesterly
12	Northwesterly

To describe the relationship between the occurrence frequency of individual circulation patterns and its corresponding frequency of generating the extreme rainfall events, Wei Yang calculated a wetness index (I_w). For this calculation, equation 1 was used.

$$I_w = \frac{R_i}{N_i} \tag{1}$$

Where R_i represents the rainfall contribution in % and N_i is the frequency of the circulation pattern in %. The wetness index can be valued as 1, < 1 and > 1 indicating normal, dry and wet conditions respectively. For example, a circulation pattern that produces a lot of precipitation but does not occur very often will have a high wetness index. The result can be seen in figure 5.

Figure 5 show that the occurrence of CP03, CP05, CP07 and CP09 may cause wet conditions, while CP11 is likely to cause dry conditions. Furthermore, CP05 appears extremely wet during the whole year while the rest of the circulation patterns that may cause wet conditions have their dominant effect in only one season. Based on the emission scenario of RCP 8.5 Wei Yang calculated the future frequencies of circulation patterns using the climate models described in section 2.6. These were used for future predictions of the hyetograph shape distribution.

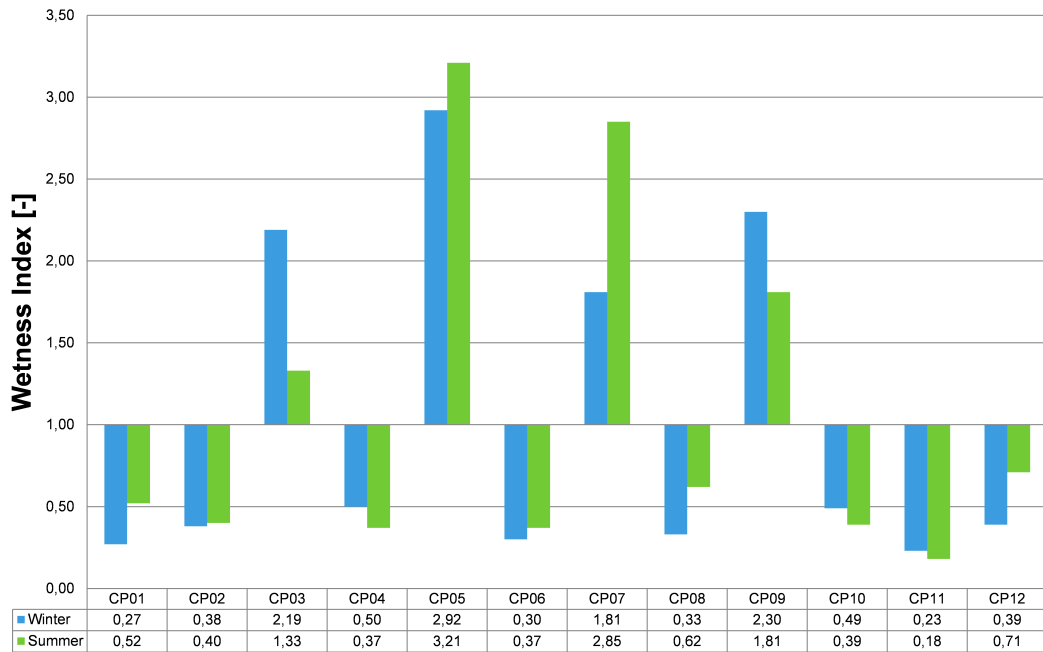|	CP01	CP02	CP03	CP04	CP05	CP06	CP07	CP08	CP09	CP10	CP11	CP12
■ Winter	0,27	0,38	2,19	0,50	2,92	0,30	1,81	0,33	2,30	0,49	0,23	0,39
■ Summer	0,52	0,40	1,33	0,37	3,21	0,37	2,85	0,62	1,81	0,39	0,18	0,71

Figure 5. Wetness index at Karlstad airport, calculated by Wei Yang at SMHI. The blue bars corresponds to the wetness index for winter months (October—April) and the green bars corresponds to the wetness index during summer months (May—September).

3.4 METHOD TO CALCULATE THE FUTURE DISTRIBUTION OF HYETO-GRAPH SHAPES

To calculate the future distribution of hyetograph shape the number of rain events between 1996–2004 were divided by how many days of the circulation pattern there were during the same period. This number represented how likely it is that for example, a cloudburst occurs when circulation pattern 5 is present and that the character of the cloudburst will look like hyetograph 3. These numbers were then multiplied by the future number of days that the circulation patterns would be present. The future number of days was a calculated mean value of the 6 climate models' different outcomes.

19

4 RESULTS
4.1 OBSERVED FREQUENCIES OF THE CIRCULATION PATTERNS
Figure 6 illustrates the frequency of each circulation pattern from 1979 to 2005. The number of days with each circulation pattern have been divided with the total number of days between 1979-2005.
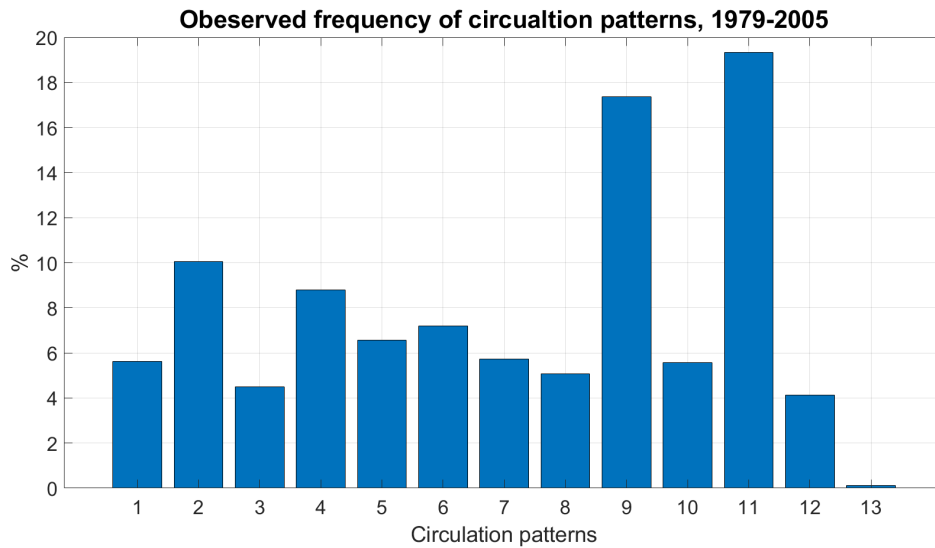

Figure 6. Frequency of the circulation patterns between 1979 and 2005.

Figure 6 show that circulation pattern 9 and 11 have the highest frequencies with 17% and 19% respectively. The unclassified circulation pattern, number 13, has a frequency of less than 1%. The remaining circulation patterns have frequencies between 4–10%. The ones with the lowest frequencies, apart from number 13, are circulation pattern 3, 8 and 12, with frequencies between 4–5%.

4.2 CIRCULATION PATTERNS' RELATION TO HYETOGRAPH SHAPE
The distribution of circulation patterns for each hyetograph was investigated by observing which circulation pattern was present the day the cloudburst occurred. To make it easier to see if there was a relation between a hyetograph shape and a specific circulation pattern the number of rain events for each circulation pattern was normalised with the total number of rain events for every hyetograph. The total number of rain events can be found in table 5. The resulting distribution of hyetograph shape for each circulation pattern is shown in figure 7 and 8. Other presentations of the data can be found in Appendix D.
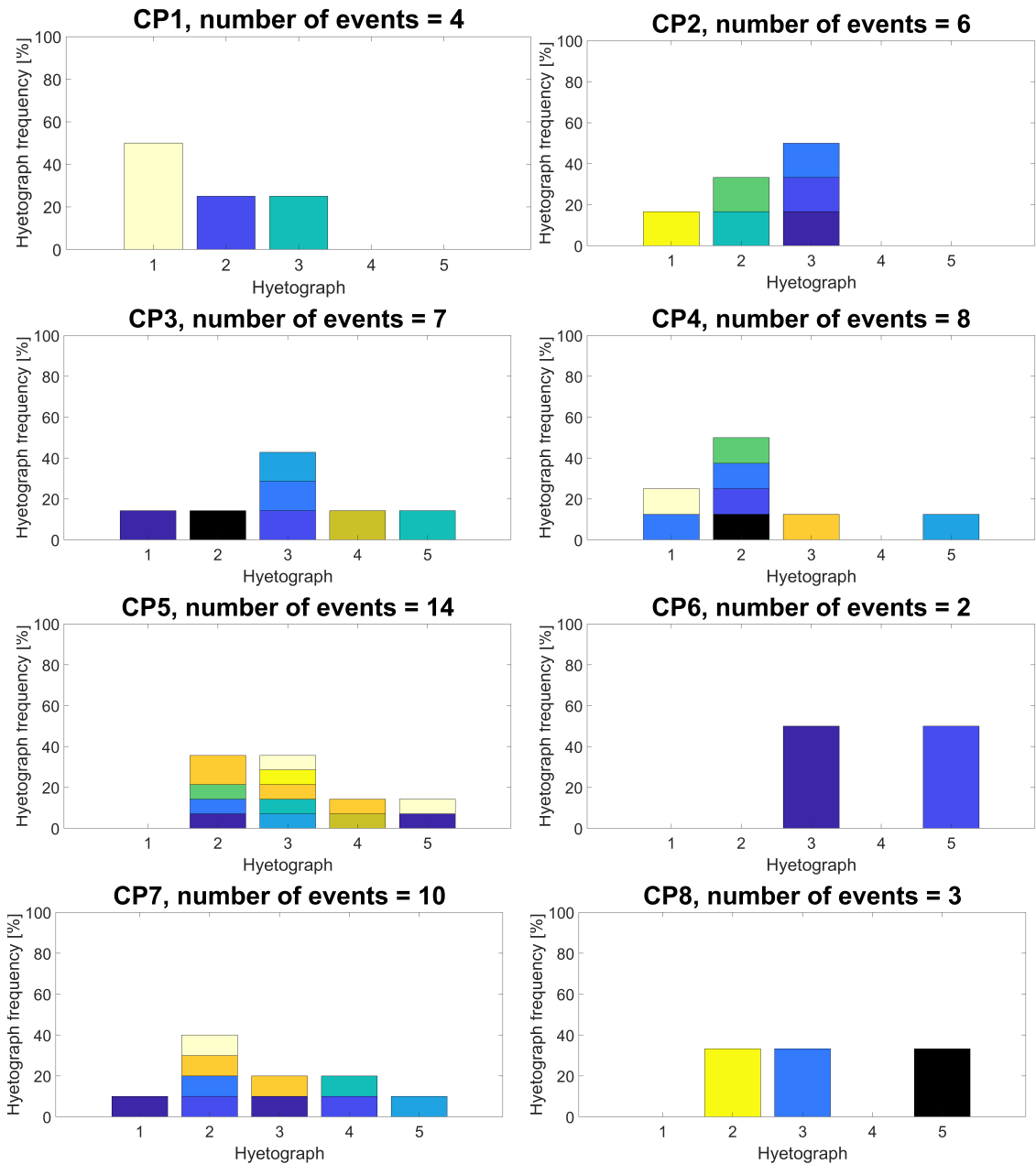
Figure 7. Normalised distribution of hyetograph shapes for circulation pattern 1–8. The colors in the bar plot corresponds to a specific station. The figures are based on rain data from 1996–2004.
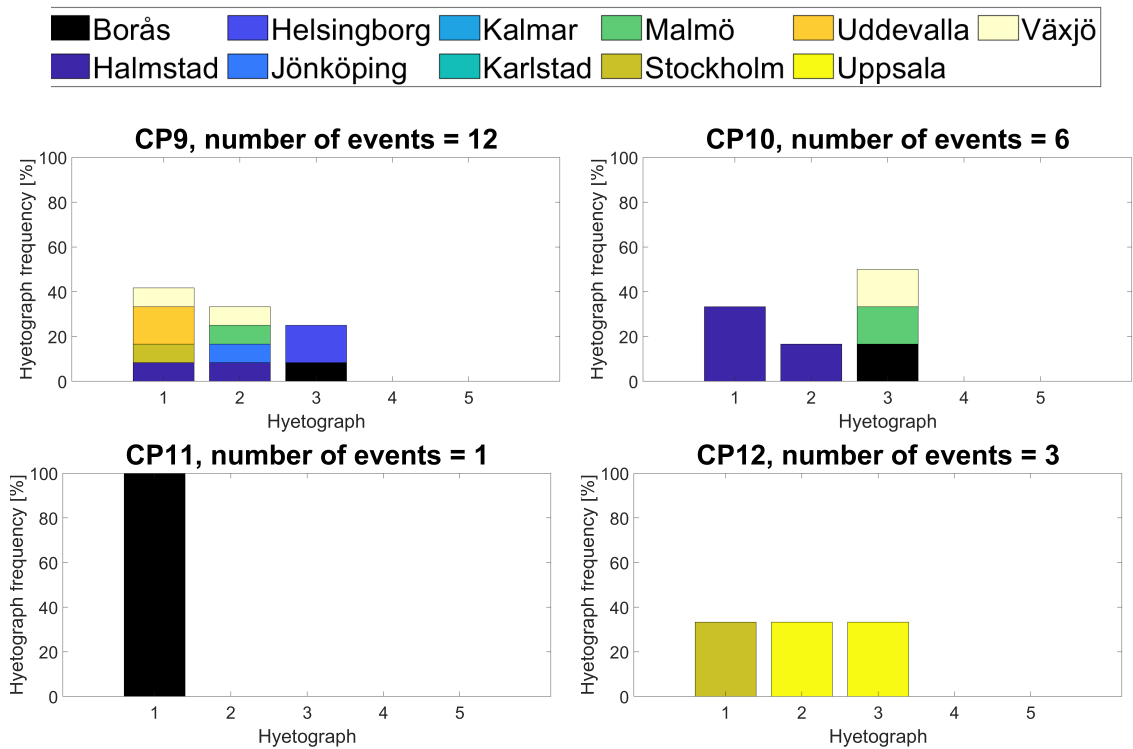
Figure 8. Normalised distribution of hyetograph shapes for circulation pattern 9–12. The colors in the bar plot corresponds to a specific station. The figures are based on rain data from 1996–2004.

From the graphs it is clear that some of the circulation patterns have too few events for any conclusions to be made. Circulation pattern 5, 7 and 9 on the other hand have between 10–12 events. At first sight it looks like these three graphs have the weight over the first two hyetographs. But compared to all other graphs, circulation pattern 5 has the largest number of hyetographs with a late rain intensity peak, i.e. hyetograph 4 and 5. The same trend can be seen when looking at the time period of 1985–2004 in figure B.2, even tough circulation pattern 9 has the same number of late peaks when looking at this time frame. Circulation pattern 9 is one of the two most common circulation patterns while circulation pattern 5 and 7 have frequencies that are about 10% lower than the frequency for circulation pattern 9, see figure 6. Therefore, it is interesting that they have almost the same number of cloudburst events. Unfortunately the number of events is too small for any robust conclusions to be made but the results can be seen as a hint of a relation.

With a number of 8 rain events, circulation pattern 4 shows an indication a connection to rains with an early peak, i.e. hyetograph 1 and 2. This trend can be seen in a similar graph but for the time period 1985–2004 in figure B.2. The number of events is still too small for any robust conclusions to be made but there is an indication of a relation and further investigation might provide results that supports this. Circulation pattern 2, 3 and 10 are difficult to say something about because of their low number of rain events but they all have their major weight at hyetograph number 3. An explanation could be that this is because hyetograph 3 is the most common hyetograph according to table 1 produced by Olsson et al. (2017).

Circulation pattern 1, 6, 8, 11 and 12 have too few rain events for any trends to been seen. This could on the other hand indicate that these circulation patterns rarely generate cloudbursts. Table 7 summarises the distribution of hyetograph shape for all circulation patterns.

Table 7. Distribution of hyetograph shape for each circulation pattern, using rain data from 1996–2004. The total number of rain events for each circulation pattern is shown in the right column.

Location	Hyetograph shape					Total number of
	1	2	3	4	5	rain events
CP01	50%	25%	25%	0%	0%	4
CP02	17%	33%	50%	0%	0%	6
CP03	14%	14%	43%	14%	14%	7
CP04	25%	50%	13%	0%	13%	8
CP05	0%	36%	36%	14%	14%	14
CP06	0%	0%	50%	0%	50%	2
CP07	10%	40%	20%	20%	10%	10
CP08	0%	33%	33%	0%	33%	3
CP09	42%	33%	25%	0%	0%	12
CP10	33%	17%	50%	0%	0%	6
CP11	100%	0%	0%	0%	0%	1
CP12	33%	33%	33%	0%	0%	3

4.3 THE CLIMATE MODELS' ACCURACY

To investigate the accuracy of the climate models their predictions of historical frequencies of the circulation patterns was compared to observed frequencies. Figure 9 illustrates how well the climate models historical predictions reflect the observed frequency of circulation patterns. The highest deviation in frequency from the observed data is for circulation pattern 3 for climate model IPSL-CM5A-MR, that is 38% lower than the observed data. This is a quite high deviation and it is probably due that it is already a low frequency. The same problem occurs for circulation pattern 12 and 13 due to their low frequencies

and their maximum deviations are 28% and 36% respectively. The other circulation patterns have frequencies from the climate models that deviate between 1% and 17% from the observed data. After discussing this result with Peter Berg at SMHI, the accuracy of the climate models was considered to be good.
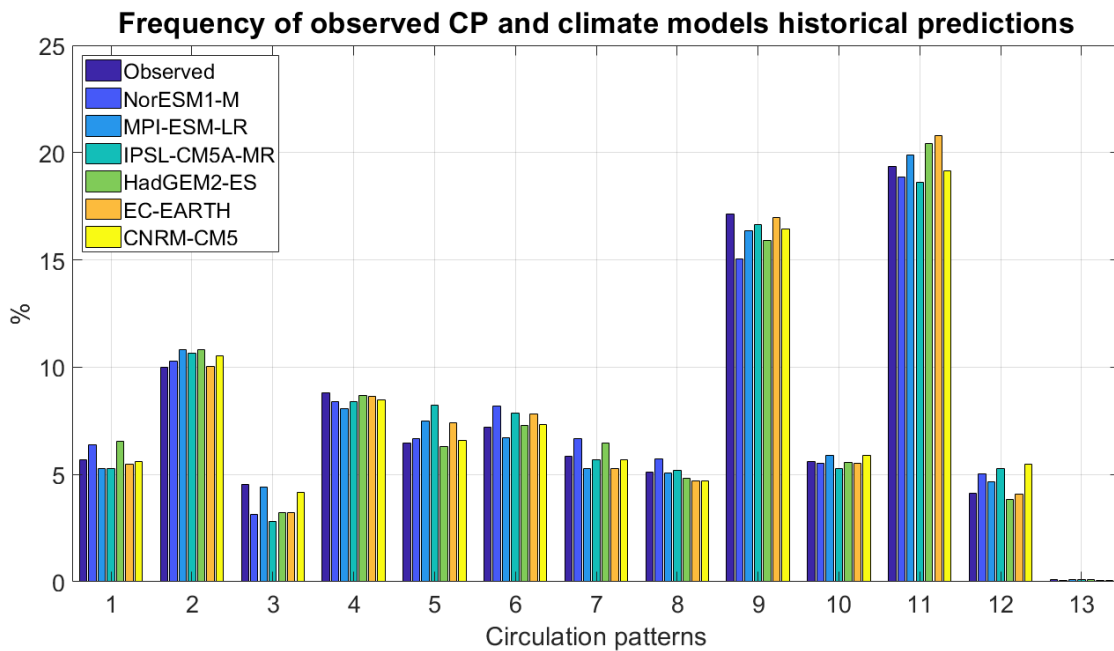

Figure 9. Comparison between the observed frequency of circulation pattern (1979–2005) and the climate models historical predictions (1979–2005), to see how well the climate models describe the real situation.

4.4 FUTURE FREQUENCIES OF CIRCULATION PATTERNS

The different climate models' future predictions of the frequencies of the circulation patterns were plotted with the time intervals 1979–2005, 2011–2040, 2041–2070 and 2071–2100, see figure 10. The calculations are based on RCP 8.5.

The climate models future prediction does not differ much from one another and there is no clear trend to be found. Although, there is a slight increase of frequency of circulation pattern 11 in all of the plots apart from the one for climate model IPSL-CM5A-MR.
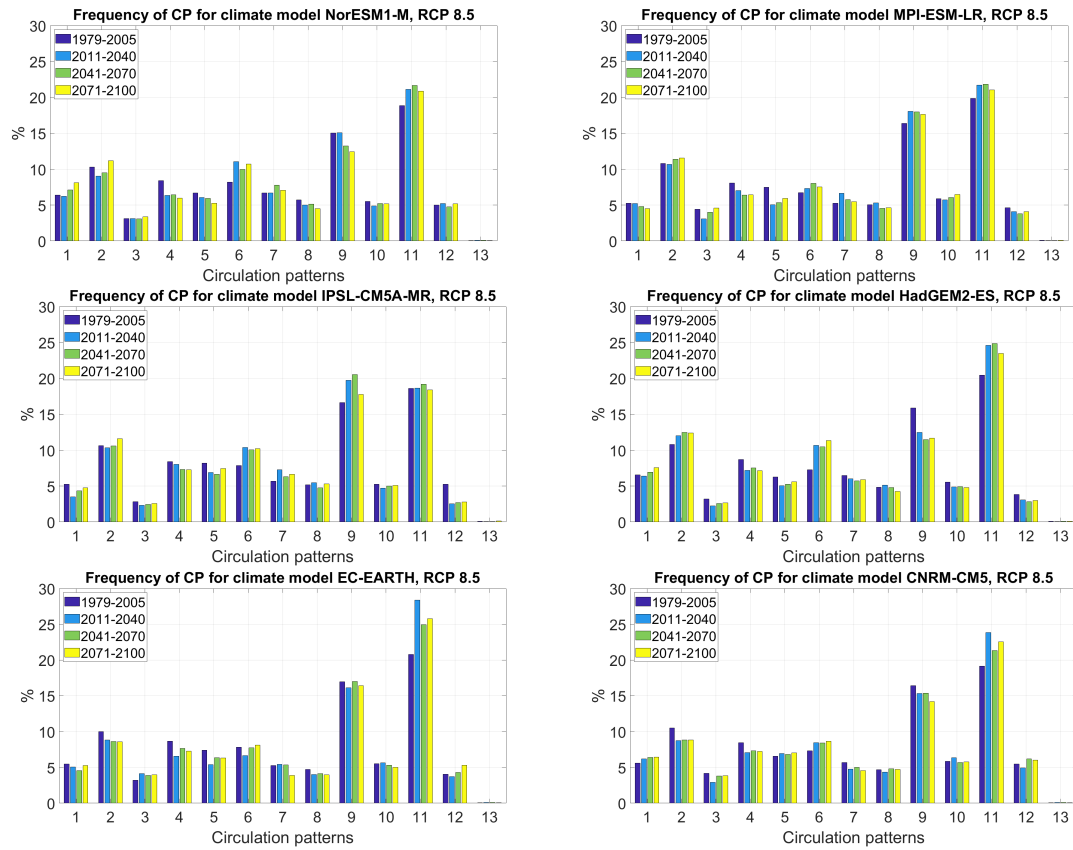
Figure 10. Historical and future frequency of circulation patterns for each climate model.

To analyse the change in frequency of the circulation patterns in the future a mean frequency for all circulation patterns for all climate models was used, these are summarised in table 8.

Table 8. The mean frequencies for future predictions by the climate models compared with observed frequencies [%]. The calculations are based on RCP 8.5.

	Circulation pattern												
	1	2	3	4	5	6	7	8	9	10	11	12	13
Observed	6	10	4	9	7	7	6	5	17	6	19	4	0
1979—2005	6	10	3	7	6	9	7	5	15	5	21	5	0
2011—2040	5	11	3	7	7	9	6	5	18	5	20	4	0
2041—2070	6	11	3	8	6	9	6	5	14	5	24	3	0
2071—2100	6	9	4	7	7	8	5	4	16	6	23	5	0

From table 8 it is difficult to see a clear trend in the frequencies of the circulation patterns. The frequencies stay within a range of 5% but they go both up and down between the time intervals. The circulation pattern with the largest change in frequency is circulation pattern 11, that goes from today´s 19% to 23%. But it is important to bear in mind that the historical predictions of circulation pattern 11 was calculated to 21% which is already 2% higher than the observed frequency. Circulation pattern 7 is supposed to decrease by 2% compared with the historical prediction. Overall the change in frequencies is very small and it is therefore, difficult to predict future trends.

4.5 FUTURE DISTRIBUTION OF HYETOGRAPH SHAPE

Table 9 show the future distribution of hyetograph shape based on the explained method in section 3.4. All calculations are based on the assumption that the likelihood for a cloudburst to occur for a certain circulation pattern will not change in the future, only the frequency of the circulation patterns.

Table 9. Future distribution of hyetograph shape, based on future frequencies of circulation patterns compared with the observed distribution when using all rain gauges.

Time period	Hyetograph shape				
	1	2	3	4	5
Observed	18.2%	27.3%	40.2%	6.1%	8.3%
1979–2005	18.7%	27.6%	39.3%	5.7%	8.7%
2011–2040	18.7%	27.1%	39.5%	5.9%	8.8%
2041–2070	18.7%	27.3%	39.5%	5.8%	8.8%
2071–2100	18.7%	27.2%	39.6%	5.6%	8.8%

First the observed distribution should be compared with the historical prediction to see how well the models and calculations reflect the observed data. The table shows that the models seem to underestimate the observed distribution for hyetograph 3 and 4, and overestimate for hyetograph 1, 2 and 5. When comparing the historically predicted distribution with future distributions it is clear that there are no notable changes to be seen in the future. Comparing the time periods 1979–2005 and 2071–2100, the frequency of hyetograph 2 will decrease with 0.4%, hyetograph 3 will increase with 0.3%, hyetograph 2 will decrease with 0.2% and hyetograph 4 decrease while hyetograph 5 increase with both 0.1%. It should be noted that this result does not say anything about increase or decrease in rain intensity of the cloudbursts in the future, only changes in the distribution between the different hyetographs.

5 DISCUSSION

5.1 CIRCULATION PATTERNS' RELATION TO HYETOGRAPH SHAPE

Based on the rain data used in this study an indication of a relation was found between circulation pattern 4 and hyetographs with an early peak, i.e. hyetograph 1 and 2. The result for circulation pattern 4, in figure 8, remained when other time periods were tested, see figure B.1. Circulation pattern 4 represents the situation of southwesterly winds in south of Sweden in combination with a low pressure over the North Atlantic Ocean. Hellström (2005) found that precipitation extremes in Sweden are favoured by southerly winds, which supports the result in this study even though the number of rain events is to small for robust conclusions to be made.

The circulation patterns with more than 8 events (see figure 8) it was difficult to see a clear relation between a specific hyetograph shape since they changed much when observing a different time period, see figure B.1. For the other circulation patterns the number of events was too small for robust conclusions to be made, see figure 8. To further investigate the relation between the hyetographs and the circulation patterns, a graph of the distribution of circulation patterns for each hyetograph was generated, see figure D.3. Something worth pointing out is that all of the hyetographs have their majority of rain events occurring when circulation pattern 5 was present, except hyetograph 1 that had 0 out of 16 events.

The relation between circulation pattern 4 and hyetograph 1 and 2 would be interesting to investigate further and a larger set of 1 min resolution rain data would give a clearer picture if there are some more relations to be found. Frequent updates of rain data from municipalities would be very useful in research like this since SMHI's automatic stations only have a time resolution of 15 min. The 15 min rain data can not capture the hyetograph shape as well as the 1 min data. For example, for a rain with a duration of 90 min the automatic station would only give 7 volumes that represent the accumulated rain within 15 min. In 2006 Hernebring (2006) pointed out that it would be preferable to have a system where municipalities continually update to the SMHI database. A system like this would be very helpful for further research on this subject and more analysis could be made on cloudbursts and their behavior. Before the decision to use data from Olsson et al. (2017) report a notable amount of time was dedicated to making contact with municipalities to get more rain data. A system like the one Hernebring (2006) presented, would be very helpful for future research.

5.2 THE CHOICE OF CIRCULATION PATTERNS

In this study 12 circulation patterns that had been optimised to represent atmospheric circulations on a North Atlantic scale for mid and south of Sweden were analysed. The method used to produce the circulation pattern classes is not the most commonly used and resulted in 12 circulation pattern classes. As discussed earlier the lack of rain data affected the result in this study and made it difficult to relations between the circulation patterns and the hyetograph shapes. A smaller number of circulation pattern classes could have increased the accuracy of the result in this study since a smaller number of circulation patterns to divide the historical cloudburst upon would increase the number of events for each circulation pattern class. When using 12 circulation patterns, as in this study, the

maximum number of rain events for a circulation pattern class was 14, which is a number that is to low for any robust conclusions to be made.

One way to lower the number of circulation pattern classes cloud be to use the more common North Atlantic circulation patterns: the North Atlantic Oscillation (NAO) with its two phases, the "blocking" and the Atlantic Ridge. On the other hand, these circulation patterns are more general while the circulation patterns used in this study were tailored for mid and south of Sweden. The amount of rain data has to be weighed against the accuracy of the circulation pattern classes to achieve an adequate amount of data to fulfill the purpose of the study. Even though the aim of this thesis was to investigate the relation between the 12 circulation pattern classes and the 5 hyetograph shapes, the number of circulation pattern classes and the method of producing them is something to bear in mind for future research to avoid shortage of rain data.

5.3 FUTURE DISTRIBUTION OF HYETOGRAPH SHAPE
The results in this study suggest that the distribution of hyetograph shape will not change considerably in the future, since the calculations in this report showed a change that is less than 1%. The calculations behind this result are based on the assumption that the likelihood of a cloudburst to occur for a certain circulation pattern will not change in the future, only the frequency of the circulation patterns. This assumption could be questioned since many studies show that with rising temperature the ability for air to hold moisture increases and therefore the frequency of heavy precipitation for each circulation pattern could change. According to IPCC (2013), heavy precipitation in northern Europe is likely to increase in frequency, intensity or both. From the result in this study, the frequency of the circulation patterns is not going to change significantly and therefore it could be an indication that the assumption of no change of frequency of cloudburst for each circulation pattern could be misleading. For future research, this aspect should be investigated.

Another aspect to have in mind when looking at the future distribution of hyetograph shape presented in this study is that the future frequencies of circulation patterns are based on the emission scenario of RCP 8.5 only. There is a risk that other frequencies could be found when looking at other emission scenarios. The decision of using only RCP 8.5 was based on the idea that it would probably have the highest effect on the atmospheric circulations and therefore, due to the time limit, only this scenario was used for the calculations of future distribution of hyetograph shape.

5.4 DEFINITION OF CLOUDBURST
Since this study is based on the hyetographs from the report by Olsson et al. (2017) the same definition of cloudburst was used. The method that was used to extract the rain events does not put an upper limit of the duration time, it only looks at when it stops raining (1 mm in 60 min was used as start and end values for the rain). Later on, the rain events with a duration of 90 min and more were grouped together. The longest rain analysed was 368 min which is a little more than 6 hours. There is a risk that the driving forces behind a rain with a duration time of 1,5 hours differ from a rain event with a duration time of 6 hours, but in this analysis they were grouped together. This could affect the analysis in

a way that unrealistic relations were found. Another approach could have been to look at the extreme rain events in terms of highest rain intensity or highest rain volume over a certain time interval. This would be interesting and perhaps show a different relation than the one presented in this study, using the same data or extending it with new data from municipalities. Something to point out in this method is that the 95th percentile probably covers more extreme rains than just cloudbursts. On the other hand, the method used by Olsson et al. (2017) to generate the hyetographs allowed rain events with a mean intensity of 6 mm/h which SMHI classifies as moderate showers (SMHI, 2015b). If the limit for a rain event to qualify as a cloudburst is to low, even moderate shower will turn up in the statistics and make the relations between cloudbursts and circulation patterns less reliable.

5.5 DISTRIBUTION OF RAIN GAUGES AND THEIR DATA SERIES

After a discussion with Peter Berg and Wei Yang at SMHI, Skellefteå and Sundsvall were excluded from the analysis due to their geographical locations in northern Sweden. The rain gauges used in this study had more similar relations between wet conditions and the circulation patterns. Even though these locations had similar wetness index graphs they can have local parameters that affect the outcome of a circulation pattern, if it becomes a cloudburst or moderate showers spread over a larger area. Cloudbursts are usually local and since the geographical distribution of rain gauges used in this study have distances of 50–150 km between each other, it is evident that cloudbursts have occurred without being registered by the rain gauges. SMHI recommends a distance of 50 km between the rain gauges to be sure that not the same rain event is captured twice. For a more reliable result it would be preferable to have an even geographical distribution of rain gauges to get a more fair relation between circulation patterns and cloudbursts. On the other hand, the rain gauges are usually located in cities and a cloudburst in a city usually causes larger damage to the society than a cloudburst in a rural area. Therefore it is probably more interesting to find the connections between the cloudbursts in the cities and their connections to the circulation patterns than covering the whole region, as this study aimed for. But it would still be preferable to have a more even distribution of rain gauges, since this would give a better understanding of the relation between cloudbursts and the circulation patterns.

Another aspect to denote is the varying frequencies of the circulation patterns between different years, see figure C.1. From these graphs it is clear that the frequencies are not stationary from year to year, even though the graphs that show a floating mean over five years indicates that there are no clear trends to be found. The result in this report is based on an 8 year period which could be affected by these fluctuations in frequencies of the circulation patterns. Therefore, it would be preferable to look at a data set with a longer running period, unfortunately this study only had access to rain data with varying starting times. After a discussion with Peter Berg, it was established that it was preferable to only use data with the same starting date. Since it was preferable to have rain data with the same starting date only 76 rain events were analysed. Figure B.1 and B.2 show the distribution when five rain gauges were selected because of their long rain data series from 1985—2004. When comparing this result with the result presented in figure 8, there are no clear differences between the different time periods. This supports the accuracy of

the results in this study, even though it is a small number of rain events.

5.6   REGIONAL DIFFERENCES

To further investigate the hyetographs' distribution, a comparison between hyetograph distribution and geographical location of the rain gauges was made, see table A.1. The table shows an indication of more frequent cloudbursts in southwest of Sweden, apart from Växjö, which is located on in the southeast of Sweden. According to this set of data, Halmstad has the highest frequency of cloudburst between 1996 and 2004. These regional differences were also pointed out by Olsson et al. (2017), where they divided Sweden into 4 regions based on their rain intensities. In their research, they used rain data with a 5 min resolution. They found that the southwest of Sweden had the highest rain intensities which this study also indicate. In their research, they used data from all of Sweden while this study only focused on mid and south of Sweden. Therefore, it would be interesting to further investigate the cloudburst distribution over all of Sweden, using tipping bucket data with 1 min resolutionn.

Another aspect of this is the result that Olsson (2019) presented in his case study where he simulated the flood depth for the different hyetographs and compared it to the most commonly used design rain when simulating rain scenarios for hydraulic modeling, the CDS-rain. He found that only hyetograph 1 were close to the flood depth of the CDS-rain. If there are regional differences, as pointed out by Olsson et al. (2017) and the result in this report, it could be interesting to further investigate if it would be preferable to use different design storms for different regions. This could not be covered in this report but would be an interesting idea for future research.

6 CONCLUSION

The aim of this study was to find a relationship between 5 hyetograph shapes and 12 atmospheric circulation pattern classes. This was investigated by looking at historical rain events and what circulation pattern was present at the day the cloudburst occurred. Furthermore, the future frequencies of those circulation patterns were studied using the result from 6 climate models. The result was used to investigate how the distribution of hyetograph shape would change in the future.

- Based on the data used in this project there is an indication of a relation between circulation pattern 4 and cloudbursts with an early peak, i.e. hyetograph 1 and 2. Circulation pattern 4 represents the situation of southwesterly winds in south of Sweden in combination with a low pressure over the Atlantic Ocean. For the rest of the circulation patterns it is difficult to see a specific relation to any of the hyetographs. With a larger set of data other relations might show and therefore this result should be seen as a hint of what the relation between those hyetographs and circulation patterns might be.

- The results in this study are based on the assumption that the likelihood of a cloudburst to occur for a circulation pattern will be the same in the future, only the frequencies of the circulation patterns might change. The climate models used in this study show that the future frequencies of the circulation patterns do not differ much from today's frequencies. Furthermore, the future distribution of hyetograph shape will not change considerably either. According to the results in this study the frequency of hyetograph 2 will decrease by less than 1% by year 2071–2100.

The conclusion of this work is that with this set of data there are some indications of a relation between southwesterly winds in south of Sweden in combination with a low pressure over the North Atlantic Ocean and hyetographs with an early peak. Even though the data set is too small for any robust conclusions to be made, this result indicates that further investigation could show interesting and useful results.

REFERENCES

Bardossy, A. och Samaniego, L. (2002). Fuzzy Rule-Based Classification of Remotely Sensed Imagery. *IEEE Transactions on Geoscience and Remote Sensing*, , vol. 40, p. 362–374, DOI: `http://dx.doi.org/10.1109/36.992798`.

Cassou, C. (2010) Euro-Atlantic regimes and their teleconnections. *Proceedings: ECMWF Seminar on Predictability in the European and Atlantic regions*. , p. 6–9.

Christiansen, B. (2007). Atmospheric Circulation Regimes: Can Cluster Analysis Provide the Number? *Journal of Climate*, , vol. 20, p. 2229–2250, DOI: `http://dx.doi.org/10.1175/JCLI4107.1`.

DMI (2017) Hvad skal du forvente, når DMI varsler skybrud?. Available from: `http://www.dmi.dk/nyheder/2018-aeldste/hvad-skal-du-forvente-naar-dmi-varsler-skybrud/` [2019-09-17].

ECMWF (2015) ENS Cluster Products. Available from: `https://www.ecmwf.int/en/forecasts/documentation-and-support/ens-cluster-products` [2019-11-12].

Elfström, C. (2015). Översvämningar kostade rekordmycket. *SVT Nyheter*.

Hellström, C. (2005). Atmospheric Conditions during Extreme and Non-Extreme Precipitation Events in Sweden. *International Journal of Climatology*, , vol. 25, p. 631–648, DOI: `http://dx.doi.org/10.1002/joc.1119`.

Hernebring, C. (2006). 10års-Regnets Återkomst, Förr Och Nu -– Regndata För Dimensionering/Kontrollberäkning Av VA-System i Tätorter.

Hernebring, C. och Mårtensson, E. (2013). Pluviala översvämningar : konsekvenser vid skyfall över tätorter, en kunskapsöversikt. *MSB567-13*, , p. 70.

IPCC (2013) *Climate Change 2013: The Physical Science Basis. Contribution of Working Group I to the Fifth Assessment Report of the Intergovernmental Panel on Climate Change*. [Stocker, T.F., D. Qin, G.-K. Plattner, M. Tignor, S.K. Allen, J. Boschung, A. Nauels, Y. Xia, V. Bex and P.M. Midgley (eds.)]. Cambridge University PressCambridge, United Kingdom and New York, NY, USA, 1535 pp.

Lamb, H. (1972). British Isles Weather Types and a Register of the Daily Sequence of Circulation Patterns 1861-1971. Her Majesty's Stationery Office.

Liljequist, G. H. (1970) *Klimatologi*. Stockholm: Generalstabens Litografiska Anstalt.

MacKay, D. J. C. (2003) Information Theory, Inference, and Learning Algorithms. *Information Theory, Inference, and Learning Algorithms*. , New York, United States: Cambridge University Press, p. 284–289.

MatLab (n.d.) K-Means Clustering. Available from: `https://se.mathworks.com/help/stats/k-means-clustering.html` [2020-01-20].

Met Office (n.d.a) North Atlantic Oscillation. Available from: `https://www.metoffice.gov.uk/weather/learn-about/weather/atmosphere/north-atlantic-oscillation` [2020-01-20].

Met Office (n.d.b) The North Atlantic Oscillation. Available from: `https://www.metoffice.gov.uk/research/climate/seasonal-to-decadal/gpc-outlooks/ens-mean/nao-description` [2020-01-20].

Met Office (n.d.c) What Are the Different Types of Rain?. https://www.metoffice.gov.uk/weather/learn-about/weather/types-of-weather/rain/types-of-rain, Available from: `https://www.metoffice.gov.uk/weather/learn-about/weather/types-of-weather/rain/types-of-rain` [2019-09-17].

Met Office (n.d.d) What Is the Jet Stream?. Available from: `https://www.metoffice.gov.uk/weather/learn-about/weather/types-of-weather/wind/what-is-the-jet-stream` [2019-09-21].

Olsson, J. (2019). The Influence of Storm Movement and Temporal Variability of Rainfall on Urban Pluvial Flooding - 1D-2D Modelling with Empirical Hyetographs and CDS-Rain.

Olsson, J., Berg, P., Eronn, A., Simonsson, L., Södling, J., Wern, L. och Yang, W. (2017). Extremregn i nuvarande och framtida klimat. *Klimatologi*, , vol. 47.

Olsson, J. och Josefsson, W. (2015). Skyfallsuppdraget -Ett Regeringsuppdrag till SMHI. *Klimatologi*, , vol. 37.

Pfahl, S. och Wernli, H. (2012). Quantifying the Relevance of Cyclones for Precipitation Extremes. *Journal of Climate*, , vol. 25, p. 6770–6780, DOI: `http://dx.doi.org/10.1175/JCLI-D-11-00705.1`.

Riahi, K., Rao, S., Krey, V., Cho, C., Chirkov, V., Fischer, G., Kindermann, G., Nakicenovic, N. och Rafaj, P. (2011). RCP 8.5—A Scenario of Comparatively High Greenhouse Gas Emissions. *Climatic Change*, , vol. 109, p. 33–57, DOI: `http://dx.doi.org/10.1007/s10584-011-0149-y`.

SMHI (2015a) Fronter | SMHI. Available from: `https://www.smhi.se/kunskapsbanken/meteorologi/fronter-1.3908` [2019-09-21].

SMHI (2015b) Nederbördsintensitet. Available from: `https://www.smhi.se/kunskapsbanken/meteorologi/nederbordsintensitet-1.19163` [2019-04-03].

SMHI (2017a) Jetströmmar | SMHI. Available from: `https://www.smhi.se/kunskapsbanken/meteorologi/jetstrommar-1.5867` [2019-09-21].

SMHI (2017b) Skyfall Och Rotblöta | SMHI. Available from: `https://www.smhi.se/kunskapsbanken/rotblota-1.17339` [2019-09-13].

SMHI (2019) Hur Fungerar En Klimatmodell? | SMHI. https://www.smhi.se/kunskapsbanken/klimat/hur-fungerar-en-klimatmodell-1.470, Available from: `https://www.smhi.se/kunskapsbanken/klimat/hur-fungerar-en-klimatmodell-1.470` [2019-12-13].

Svenskt Vatten (2011). Nederbördsdata Vid Dimensionering Och Analys Av Avloppssystem. *P104*.

Willems, P., Arnbjerg-Nielsen, K., Olsson, J. och Nguyen, V. (2012). Climate Change Impact Assessment on Urban Rainfall Extremes and Urban Drainage: Methods and Shortcomings. *Atmospheric Research*, , vol. 103, p. 106–118, DOI: `http://dx.doi.org/10.1016/j.atmosres.2011.04.003`.

Yiou, P. och Nogaj, M. (2004). Extreme Climatic Events and Weather Regimes over the North Atlantic: When and Where? *Geophysical Research Letters*, , vol. 31, DOI: `http://dx.doi.org/10.1029/2003GL019119`.

UNPUBLISHED REFERENCES
Yang, W. (2019). Private communication.

APPENDIX

Appendix A Distribution of hyetograph shape for each location

Table A.1 show The distribution of hyetograph shape and frequency of cloudburst for 13 of the 15 locations, only using rain data from 1996–2004.

Table A.1. Distribution of hyetograph shape for the chosen locations. The table also show the frequency of cloudburst in each location based on the time period of 8 years.

Location	Hyetograph shape					Total number of rain events	Frequency of cloudbursts
	1	2	3	4	5		
Borås	17%	33%	33%	0%	17%	6	0.75
Halmstad	42%	25%	25%	0%	8%	12	1.50
Helsingborg	0%	33%	44%	11%	11%	9	1.13
Jönköping	13%	50%	38%	0%	0%	8	1.00
Kalmar	0.0%	0.0%	50%	0.0%	50%	4	0.5
Karlstad	0%	20%	40%	20%	20%	5	0.63
Malmö	0%	80%	20%	0%	0%	5	0.63
Skellefteå	0%	0%	100%	0%	0 %	4	0.5
Stockholm	50%	0%	0%	50%	0.0 %	4	0.5
Sundsvall	25%	50%	25%	0%	0 %	4	0.5
Uddevalla	22%	33%	33%	11%	0 %	9	1.13
Uppsala	20%	40%	40%	0%	0 %	5	0.63
Växjö	44%	22%	22%	0%	11%	9	1.13

Appendix B Distribution of hyetograph shape for different time series

To investigate the distribution over at fixed number of year five locations were chosen: Borås, Jönköping, Malmö, Stockholm and Växjö, due to their long time series. Figure B.1 and B.2 show the distribution of hyetograph shape for each circulation pattern, using only these locations with rain data from year 1985 to 2004. The bar plots were normalised with total number of rain events for each hyetograph shape, these can be seen in table B.1.

Table B.1. Distribution of hyetograph shape of the rain events using rain data from 1985 to 2004 (19 years).

Duration time	Hyetograph shape					Total number of
[min]	1	2	3	4	5	rain events
>90	9	20	23	4	6	57
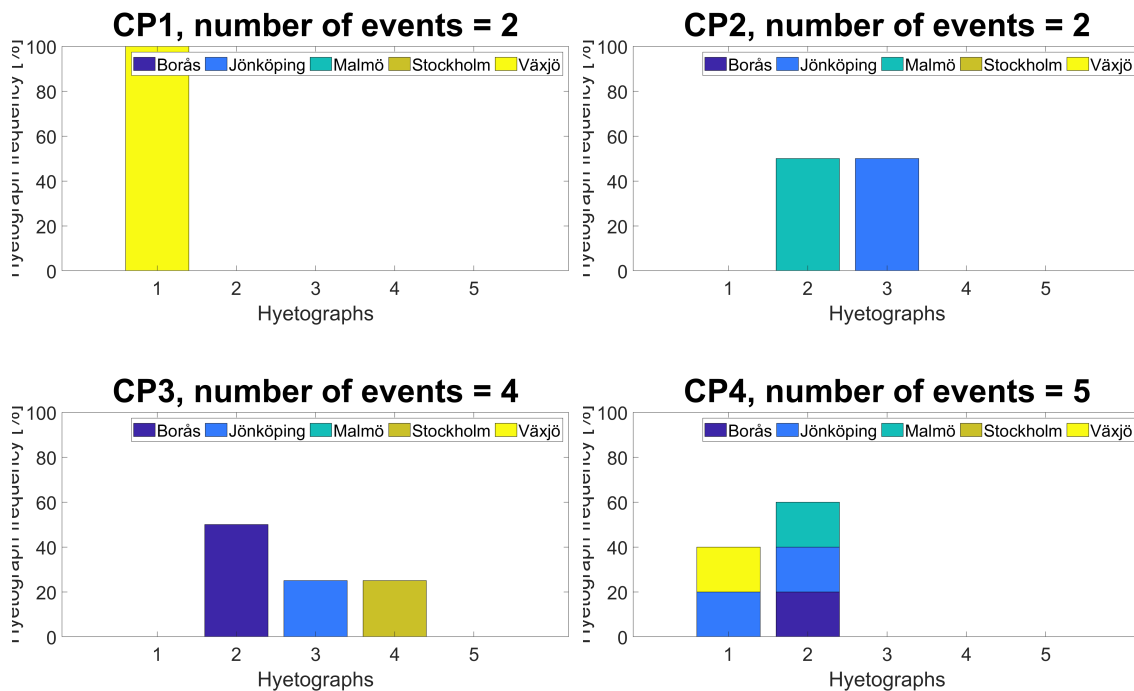
Figure B.1. Normalised distribution of hyetograph shapes for circulation pattern 1–4, from year 1985–2004. Each color in the bar plot corresponds to a specific station.
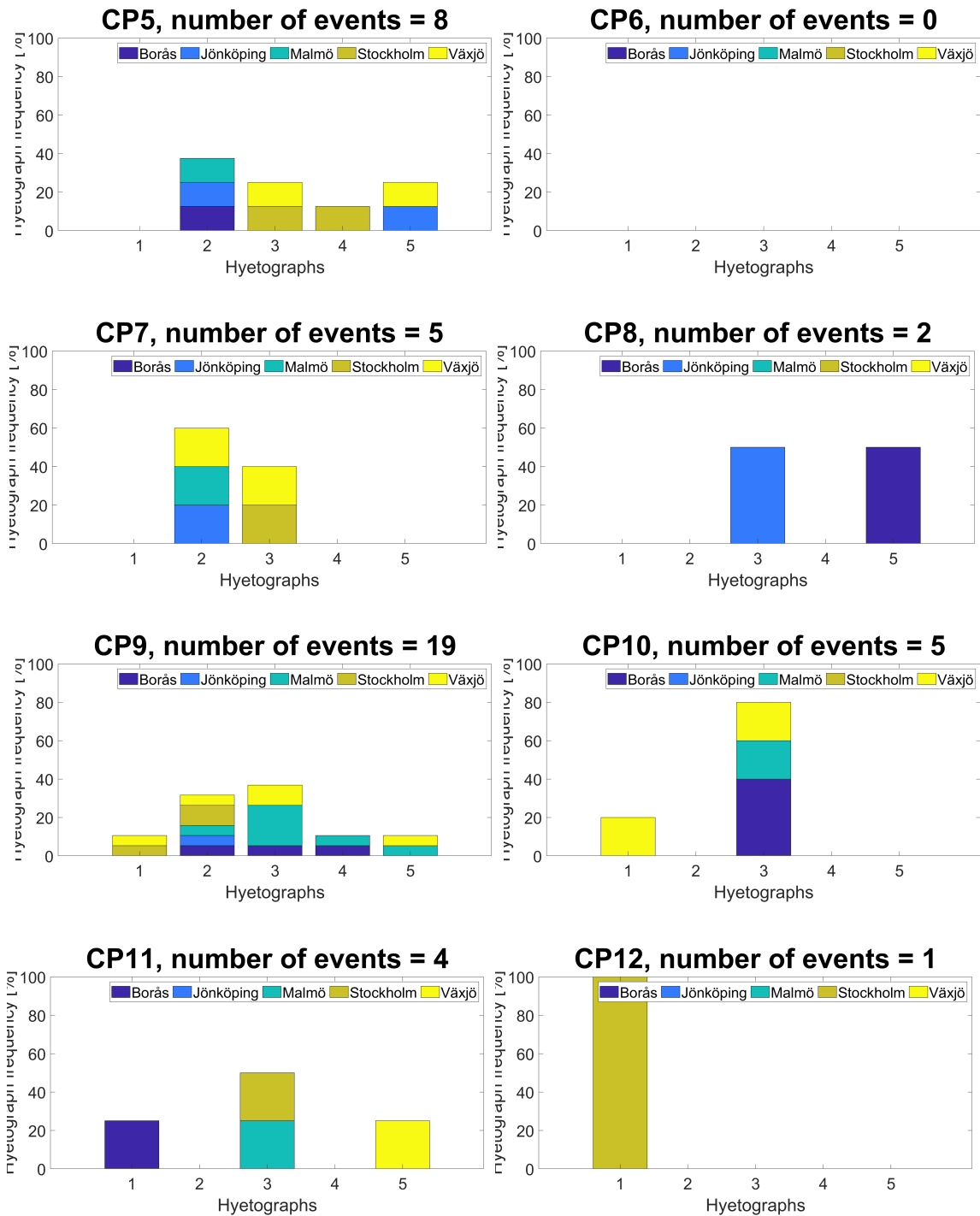
Figure B.2. Normalised distribution of hyetograph shapes for circulation pattern 5–12, from year 1985–2004. Each color in the bar plot corresponds to a specific station.

Appendix C Observed frequency change of circulation patterns, 1980-2004

To better understand how the frequency of the circulation patter changes during seasons and between different years the observed frequencies between year 1980–2004 were plotted for each year. Together with those frequencies the number of cloudburst in relation to how many rain gauges running at that time was plotted and is market with a dotted red line, see figure C.1. The number of cloudburst were divided by the number of stations to get a relation. Since the frequencies varies much between the every year a moving mean was calculated to make it easier to see trends, these are the second and fourth plot.
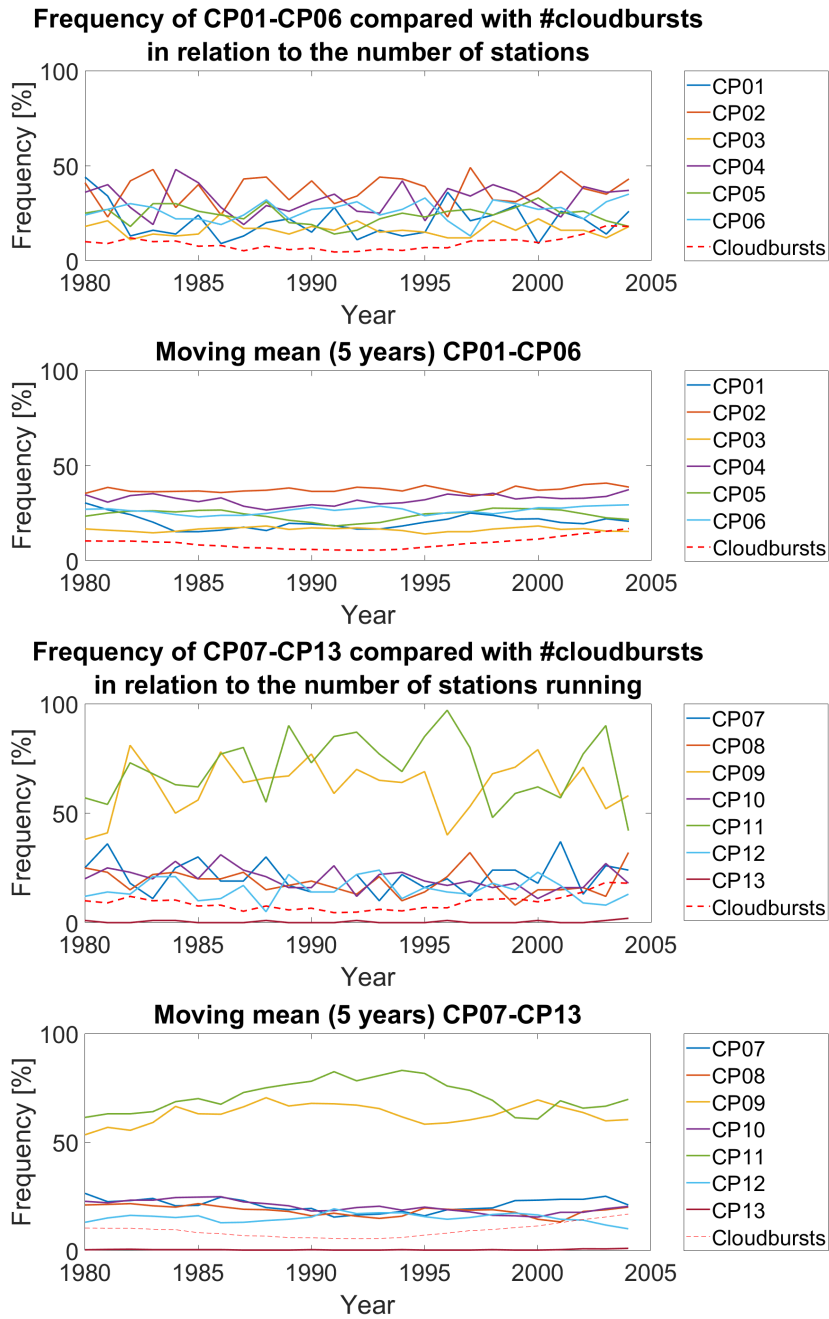
Figure C.1. Frequency changes between different years of the circulation patterns, in plot 1 and 3. In plot 2 and 4 a moving mean was applied to smooth out the lines to make it easier to see any trends. The red dotted line illustrates the number of cloudbursts divided by the number of stations running at that time.

From figure C.1 it is clear that the frequency vary significantly between different years. Circulation pattern 9 and 11 have had much higher frequencies than the other circulation patterns over all the analysed years. There are no other clear trends to be found in this result.

Appendix D Distribution of hyetograph shape for each circulation pattern 1996–2004, other presentations

The bar-plots have been normalised with the total number of rain event for each hyetograph, which means that the bars that represent the distribution for example hyetograph 1 ads up to 100% if they are added with the bars for hyetograph 1 in the other bar plots.

Table D.1. Distribution of hyetograph shape of the rain events. The total number of rain events is shown in the right column.

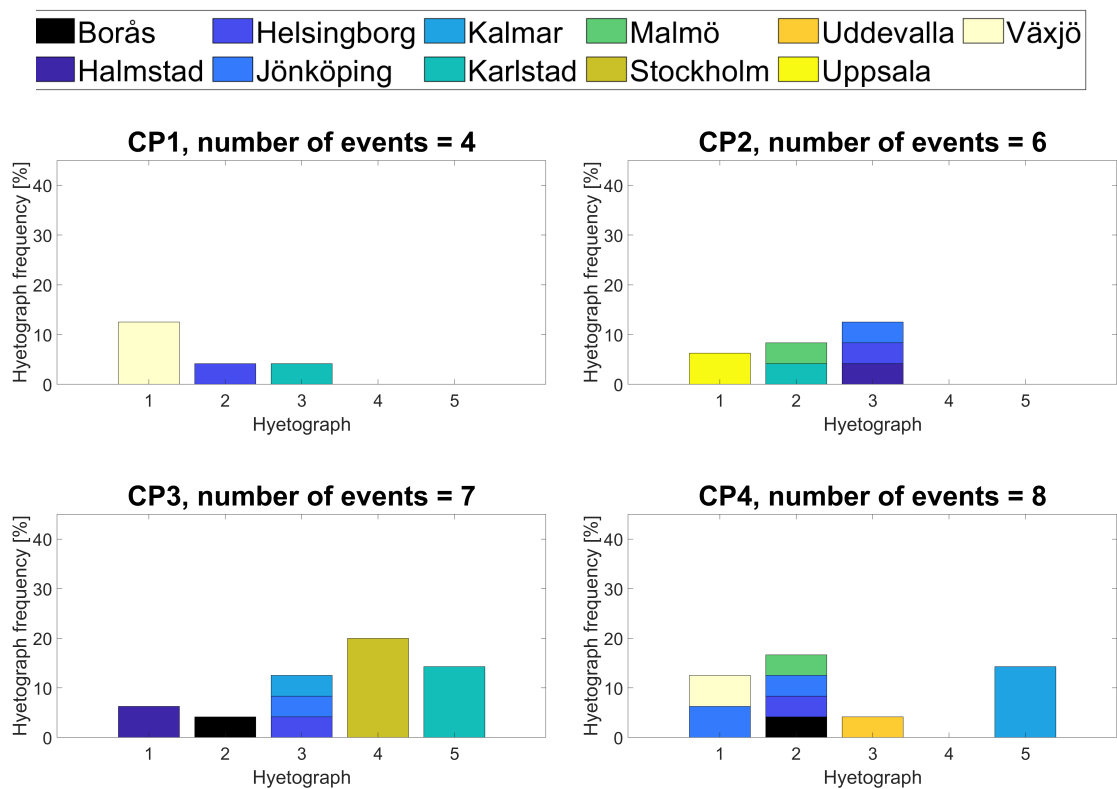| Duration time	Hyetograph shape					Total number of
[min]	1	2	3	4	5	rain events
>90	16	24	24	5	7	76

Figure D.1. Normalised distribution of hyetograph shapes for circulation pattern 1–4, from year 1996-2004. The colors in the bar plot corresponds to a specific station.
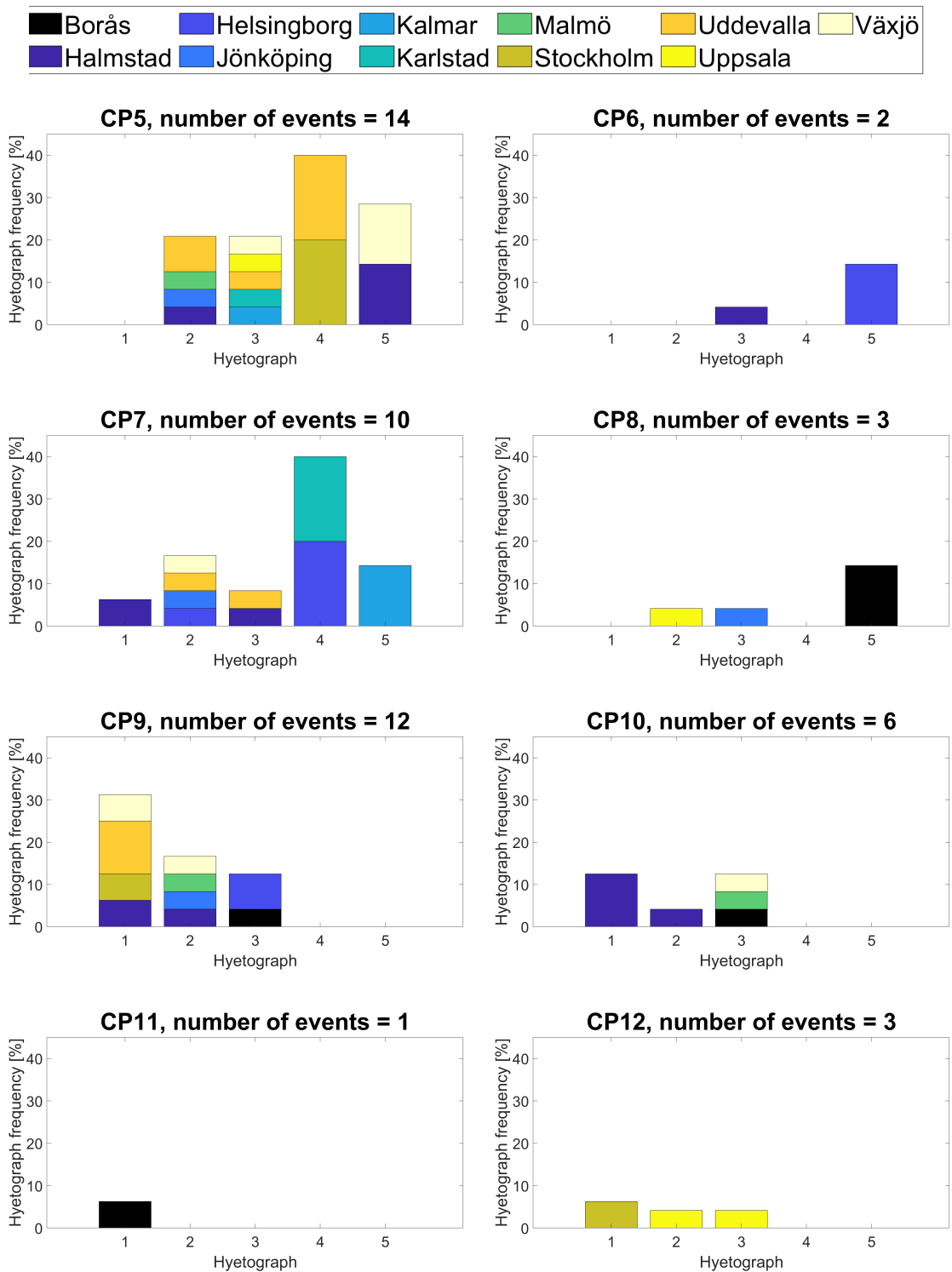
Figure D.2. Normalised distribution of hyetograph shapes for circulation pattern 5–12, form year 1994–2004. The colors in the bar plot corresponds to a specific station.
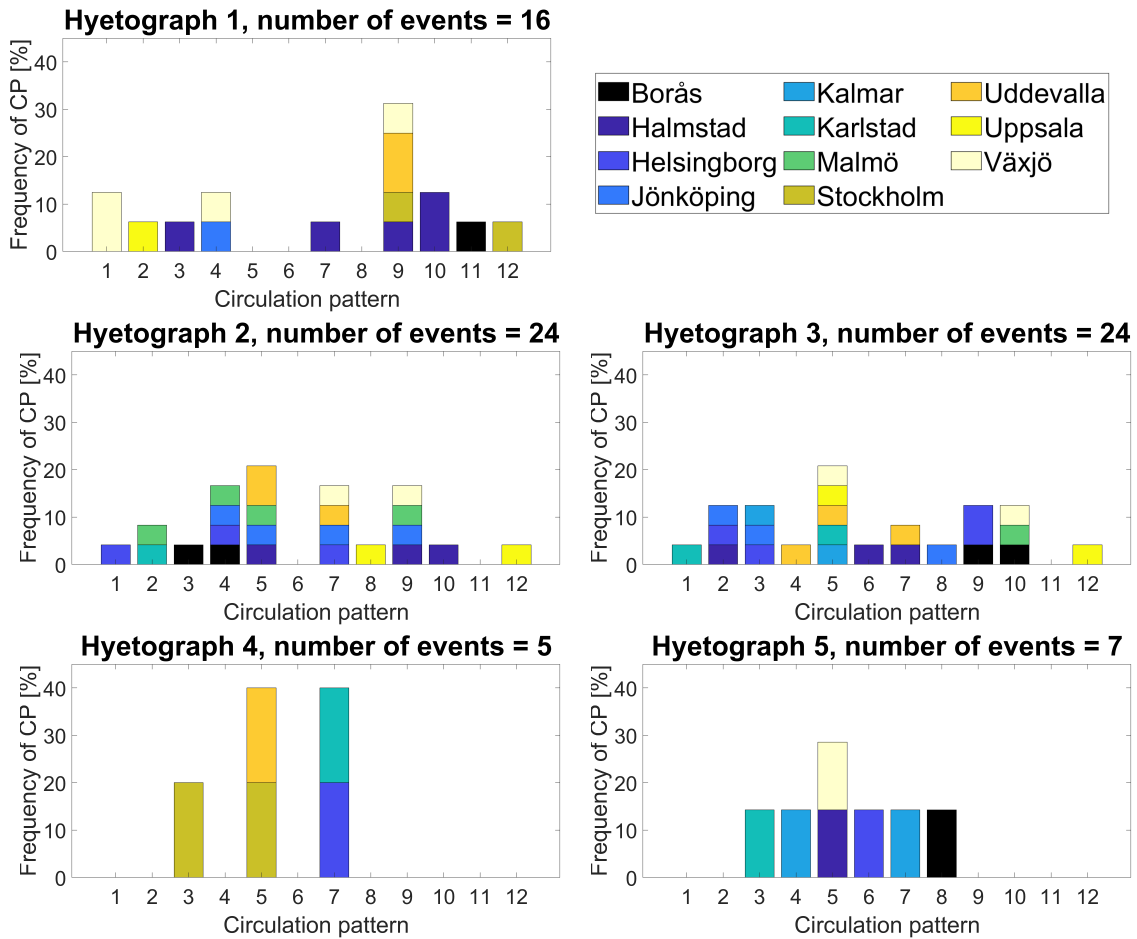
41

Figure D.3. Distribution of circulation patterns for each hyetograph shape. The graphs have been normalised with total number of events for each hyetograph.